

pubs.acs.org/JACS Article

Synthesis of Crystallographically Characterizable Bis(cyclopentadienyl) Sc(II) Complexes: (C₅H₂^tBu₃)₂Sc and {[C₅H₃(SiMe₃)₂]₂ScI}¹⁻

Joshua D. Queen, Lauren M. Anderson-Sanchez, Cary R. Stennett, Ahmadreza Rajabi, Joseph W. Ziller, Filipp Furche,* and William J. Evans*



Cite This: https://doi.org/10.1021/jacs.3c11922



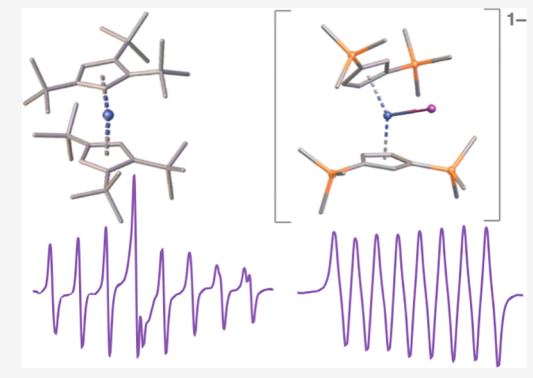
ACCESS I

III Metrics & More

Article Recommendations

s Supporting Information

ABSTRACT: The synthesis of previously unknown bis(cyclopentadienyl) complexes of the first transition metal, i.e., Sc(II) scandocene complexes, has been investigated using $C_5H_2(^tBu)_3$ (Cp^{ttt}), C_5Me_5 (Cp^*), and $C_5H_3(SiMe_3)_2$ (Cp'') ligands. Cp^{ttt}_2ScI , **1**, formed from ScI₃ and KCp^{ttt}, can be reduced with potassium graphite (KC₈) in hexanes to generate dark-red crystals of the first crystallographically characterizable bis(cyclopentadienyl) scandium(II) complex, Cp^{ttt}_2Sc , **2**. Complex **2** has a 170.6° (ring centroid)-Sc-(ring centroid) angle and exhibits an eight-line EPR spectrum characteristic of Sc(II) with A_{iso} = 82.6 MHz (29.6 G). It sublimes at 200 °C at 10^{-4} Torr and has a melting point of 268–271 °C. Reductions of Cp^*_2ScI and Cp''_2ScI under analogous conditions in hexanes did not provide new Sc(II) complexes, and reduction of Cp^*_2ScI in benzene formed the Sc(III) phenyl complex, Cp^*_2ScI (C_6H_5), **3**, by C–H bond activation. However, in Et₂O and toluene, reduction of Cp^*_2ScI at



-78 °C gives a dark-red solution, 4, which displays an eight-line EPR pattern like that of 1, but it did not provide thermally stable crystals. Reduction of Cp"₂ScI, in THF or Et₂O at -35 °C in the presence of 2.2.2-cryptand, yields the green Sc(II) metallocene iodide complex, [K(crypt)][Cp"₂ScI], 5, which was identified by X-ray crystallography and EPR spectroscopy and is thermally unstable. The analogous reaction of Cp*₂ScI with KC₈ and 18-crown-6 in Et₂O gave the ligand redistribution product, [Cp*₂Sc(18-crown-6- κ^2 O,O')][Cp*₂ScI₂], 6, as the only crystalline product. Density functional theory calculations on the electronic structure of these compounds are reported in addition to a steric analysis using the Guzei method.

INTRODUCTION

Although scandium is the first member of the transition metal series, development of its chemistry has lagged behind that of the other transition metals. This is often attributed to the inherent experimental difficulties with the electropositive Sc(III) ion and the high reactivity of its lower oxidation states. He was not until 1998 that a heteroatomic scandium metallocene, $Sc(P_2C_3^tBu_3)_2$, was reported by Cloke et al. from the metal vapor reaction of Sc with $^tBuC \equiv P$, eq 1.

$$Sc_{(vapor)} + {}^{t}BuC \equiv P \xrightarrow{^{t}Bu} {}^{t}Bu \xrightarrow{^{t}Bu} \xrightarrow{^{t}Bu} {}^{t}Bu \xrightarrow{^{t}Bu} \xrightarrow{^{t}Bu} {}^{t}Bu \xrightarrow{^{t}Bu} \xrightarrow{^{t}B$$

This complex formed in low yield alongside the previously reported Sc(I) complex $[\{(\eta^5-P_3C_2^tBu_2)Sc\}_2(\mu-\eta^6:\eta^6-\eta^6-\eta^6)]$

 $P_3C_3^tBu_3$],³ but the high reactivity of $Sc(P_2C_3^tBu_3)_2$ did not allow for its crystallographic characterization. It was not until 2017 that the first X-ray crystal structure of a molecular Sc(II) complex, the $\{Sc[N(SiMe_3)_2]_3\}^{1-}$ anion, appeared in the literature $(eq\ 2)$.⁵ A second example, the $[Sc(OC_6H_2-2,6-^tBu_2-4-Me)_3]^{1-}$ anion, was reported in 2018.⁶

Received: October 25, 2023 Revised: December 20, 2023 Accepted: December 22, 2023



A major advance in rare-earth element metallocene chemistry occurred recently when the results of Sitzmann a n d co-workers in 2000 on bis-(pentaisopropylcyclopentadienyl) metallocenes, $\operatorname{Cp^{iPrS}}_2\operatorname{Ln}(\operatorname{Cp^{iPrS}}=\operatorname{C_5^iPr_5})$ of Ln = Sm, Eu, and Yb, were expanded by McClain et al. to yttrium and the rest of the lanthanide series, Ln = Y, La, Ce, Pr, Nd, Gd, Tb, Dy, Ho, Er, Tm, and Lu, cxcluding radioactive Pm. This demonstrated the power of sterically bulky ligands to trap highly reactive rare-earth metals in low oxidation states as Cloke and co-workers had done in the 1980s with the Ln(0) complexes, $^{1,12,13}(\operatorname{C_6H_3^tBu_3})_2\operatorname{Ln}$, for Ln = Sc, Y, Nd, Gd, Tb, Dy, Ho, Er, and Lu.

The importance of steric protection demonstrated by these results and the prevalence of three *tert*-butyl substituents on the rings of these low valent rare-earth metallocenes such as $Sc(P_2C_3{}^tBu_3)_2{}^4$ and $(C_6H_3{}^tBu_3)_2Ln^{1,12,13}$ led us to attempt the synthesis of the tri-*tert*-butyl-substituted cyclopentadienyl Sc(II) complex, Cp^{ttt}_2Sc $(Cp^{ttt}=C_5H_2{}^tBu_3)$. Previously, Nief et al. had shown the utility of the Cp^{ttt} ligand in generating isolable $Dy(II)^{14}$ and $Nd(II)^{15}$ complexes, $[Cp^{ttt}_2Ln(\mu-X)K(18\text{-crown-6})]$ $(Ln=Dy, X=BH_4, Br, I; Ln=Nd, X=I)$, eq 3, and the Cp^{ttt} ligand has proven valuable with other

systems as well.^{16–26} Furthermore, bulky alkyl groups have been found to impart extra stability to certain organometallic compounds through attractive interligand dispersion force effects.^{27,28}

The reduction of Ln(III) precursors in noncoordinating solvents (e.g., alkane and aromatic hydrocarbons) has proven a successful strategy for the synthesis of $\mathrm{Cp^{iPr5}_2Ln},^{10,11}$ as well as the Tm(II) compound $\mathrm{Cp^{ttt}_2Tm}.^{18}$ Following this protocol, we report the isolation of the first crystallographically characterizable bis(cyclopentadienyl) Sc(II) complex, $\mathrm{Cp^{ttt}_2Sc}.$ This finally extends this classic set of bis(cyclopentadienyl) organometallic complexes^{29,30} to scandium, the first metal of the transition series and the lightest of the rare-earth elements. The characteristic EPR and UV—visible spectra of this complex are reported as well as density functional theory calculations describing the electronic structure. To investigate the importance of the substituents on the cyclopentadienyl ligands, reactions with the $\mathrm{C_5Me_5}$ and $\mathrm{C_5H_3(SiMe_3)_2}$ ligands were also examined and the resulting new Sc(II) complexes are described.

RESULTS

Sc(II) with C₅H₂(^tBu)₃ (Cp^{ttt}). Cp^{ttt}₂ScI, 1. The precursor desired for the synthesis of Cp^{ttt}₂Sc, namely, Cp^{ttt}₂ScI, was prepared by heating a mixture of two equiv of KCp^{ttt} and ScI₃ in toluene at reflux for 3 days. Removal of solvent under reduced pressure followed by extraction with hexanes and subsequent evaporation of the hexane gave the yellow complex Cp^{ttt}₂ScI, 1, in 34% yield. The molecular structure of 1 (Figure 1), was confirmed by X-ray diffraction of crystals of 1, grown

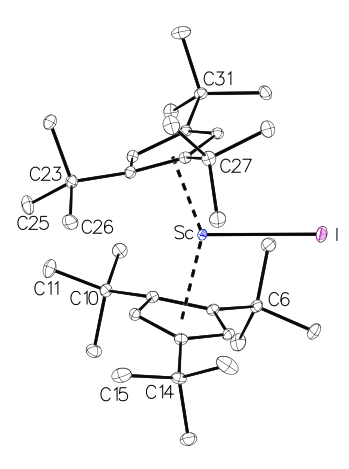


Figure 1. Molecular structure of Cp^{ttt}_2ScI , 1, with thermal ellipsoids drawn at the 50% probability level; hydrogen atoms not shown for clarity.

by storing a toluene solution at $-35\,^{\circ}\mathrm{C}$ for 2 days. Complex 1 was found to be stable up to at least 260 $^{\circ}\mathrm{C}$ without melting or decomposition and could be sublimed at 230 $^{\circ}\mathrm{C}$ and $10^{-4}\,^{\circ}\mathrm{C}$ Torr. MALDI-TOF MS using an anthracene matrix did not show the parent ion, $[\mathrm{Cp^{ttt}}_2\mathrm{ScI}]^+$, but instead fragmentation was observed with loss of the $\mathrm{Cp^{ttt}}$ and I ligands. In positive ion mode, the $[\mathrm{Cp^{ttt}}\mathrm{ScI}]^+$, $[\mathrm{Cp^{ttt}}\mathrm{Sc}(\mathrm{anthracene})]^+$, and $[\mathrm{Cp^{ttt}}\mathrm{2sc}]^-$ ions were identified, while in negative ion mode the $[\mathrm{II}]^-$, $[\mathrm{Cp^{ttt}}]^-$, $[\mathrm{Sc}(\mathrm{anthracene})\mathrm{I_2}]^-$, $[\mathrm{ScI_3}]^-$, and $[\mathrm{Cp^{ttt}}\mathrm{ScI_2}]^-$ fragments were seen.

Complex 1 has a 147.0° (Cp^{ttt} ring centroid)–Sc–(Cp^{ttt} ring centroid) angle that is wider than the 140.51(8)° angle of the pentamethylcyclopentadienyl analogue, Cp* $_2$ ScI. 31 Both the 2.8569(3) Å Sc–I distance and the 2.233(1) and 2.224(1) Å Sc–(Cp^{ttt} ring centroid) distances are longer than those of Cp* $_2$ ScI: Sc–I, 2.8194(3), and Sc–(Cp* ring centroid), 2.16(1) Å. The two similar (Cp^{ttt} ring centroid)–Sc–I angles in 1, 105.9° and 107.1°, show that the iodide is located midway between the rings as is typical in bis(cyclopentadienyl)Ln^{III} halides. The top view of the complex (Figure 2) shows the

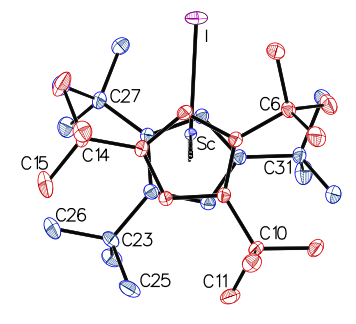


Figure 2. Top view of Cp^{ttt}_2ScI , 1, with ellipsoids shown at 50% probability and hydrogen atoms not shown for clarity. The Cp^{ttt} ligands are color coded: red above Sc and blue below Sc.

arrangement of the iodide with respect to the *tert*-butyl groups. The closest measured distance between the *tert*-butyl groups on separate cyclopentadienyl rings is the 2.00 Å separation of H15A and H26A on C15 and C26, respectively. This is less than twice the 1.2 Å van der Waals radius of hydrogen.³² Additionally, the closest C···C distance between *tert*-butyl groups is the 3.582(3) Å separation between the C11 and C25 methyl groups, which is less than twice the 2.0 Å van der Waals

radius of a methyl group.³² Such short intramolecular separations can be indicative of attractive interligand dispersion force interactions in organometallic molecules.^{27,28}

Cpttt2Sc, 2. Treatment of Cpttt2ScI with KC8 in hexane at room temperature under an argon atmosphere for 6 days resulted in a gradual color change from yellow to dark red. The dark precipitates (presumably graphite and KI) were separated by centrifugation followed by filtration and removal of the solvent from the supernatant gave Cpttt2Sc, 2, as a dark red powder in ca. 75% yield (eq 4). Recrystallization from hexane at room temperature overnight provided X-ray quality crystals of 2, shown in Figures 3 and 4.

$${}^{t}Bu$$

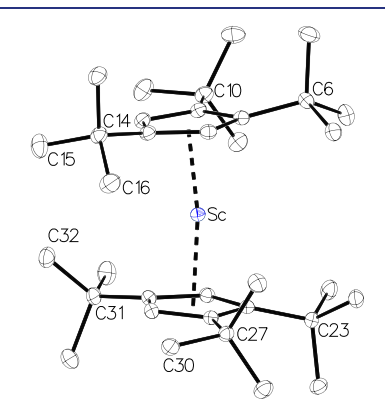


Figure 3. Molecular structure of Cpttt2Sc, 2, with thermal ellipsoids drawn at the 50% probability level and hydrogen atoms not shown for clarity.

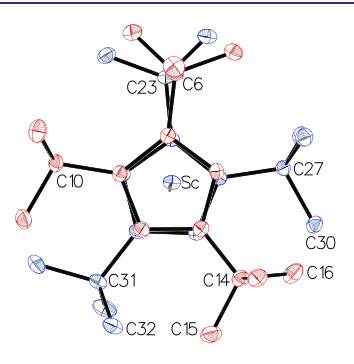


Figure 4. Top view of Cpttt2Sc, 2, with ellipsoids shown at 50% probability and hydrogen atoms not shown for clarity. The Cpttt ligands are color coded: red above Sc and blue below Sc.

The EPR spectra of toluene and hexane solutions of Cpttt 2Sc at 298 K both displayed eight-line patterns due to coupling to the Sc center (45 Sc, I = 7/2, 100% abundance). Additional signals were initially observed in the spectra, but sublimation of 2 at 200 $^{\circ}$ C and 10^{-4} Torr gave material that displayed a cleaner eight-line pattern (Figure 5), with $g_{iso} = 1.99$ and a hyperfine coupling constant of $A_{iso} = 82.6$ MHz (29.6 G) calculated from an isotropic simulation using EasySpin.³³ The

spectrum appears to have some anisotropy at ambient temperature that was consistent across multiple samples independent of choice of solvent. At 77 K, the spectrum displays only a broad signal with unresolved hyperfine coupling. Additional EPR spectra are shown in the Supporting Information. For comparison, EPR spectra reported for $Sc(P_2C_3^tBu_3)_2$ at 120 K, $\{Sc[N(SiMe_3)_2]_3\}^{1-}$ at 298 K, and $Sc(OC_6H_2-2,6^{-t}Bu_2-4-Me)_3]^{1-}$ at 77 K have g_{iso} values of 1.98, 1.977, and 2.01 respectively, and A_{iso} values of 103 MHz (37) G), 592 MHz (214 G), and 819 MHz (291 G) respectively. These values are summarized in Table 1.

The Evans method^{34–36} magnetic susceptibility measurement on Cpttt 2Sc indicated a magnetic moment of 1.9 µB, which is consistent with one unpaired electron as expected for a 3d¹ electron configuration for the Sc(II) ion. The UV-visible spectrum of 2, shown in Figure 6, has an absorbance maximum at 520 nm and is discussed further in the Computational Analysis.

Complex 2 is a bis(cyclopentadienyl) Sc(II) complex like ferrocene (i.e., a scandocene), but unlike ferrocene, the rings are not rigorously parallel: the (Cpttt ring centroid)-Sc-(Cpttt ring centroid) angle is 170.6°, a feature that is discussed below in detail in Computational Analysis. The 2.154(1) Å and 2.156(1) Å Sc-(Cpttt ring centroid) distances are smaller than those of Cpttt2ScI by about 0.07 Å, which is in the range expected for the difference between six and seven coordinate scandium complexes using Shannon radii.³⁷ The arrangement of the six tert-butyl groups on the two ligands is such that four are staggered and two are eclipsed, as shown by the top view in Figure 4. The eclipsed groups are distorted out of the plane of the cyclopentadienyl rings, with the quaternary carbons C6 and C23 lying 0.322 and 0.308 Å above the mean plane of the five cyclopentadienyl ring carbon atoms. In comparison, the other quaternary carbons lie distances of 0.194 (C31), 0.252 (C14), 0.034 (C27), and 0.022 Å (C10) from the cyclopentadienyl planes. All of these displacements are less than the 0.48 Å displacement for the carbon of methyl substituents in (C₅Me₅)₃M complexes that display sterically induced reduction chemistry.³⁸ The closest approaches between methyl groups of any two tert-butyl substituents are the 3.922(2) Å C15···C32 and 4.007(2) Å C16···C30 separations, which are close to the 4.0 Å sum of van der Waals radii of two methyl groups.³² The closest C(methyl)...Sc approaches are the 3.558(1) Å C11···Sc and 3.476(1) Å C28···Sc distances. These values are much longer than the 2.524(10) Å $\text{Ti} \cdots \beta$ carbon distance in EtTiCl₃(Me₂P(CH₂)₂PMe₂), which has an agostic interaction.^{39,40}

Cpttt2Sc shows exceptional thermal stability: it can be sublimed at 10⁻⁴ Torr and 200 °C, and the crystals melt without decomposition at 268-271 °C. The MALDI-TOF mass spectrum of 2 using an anthracene matrix shows only the parent ion $[Cp^{ttt}_2Sc]^+$ at 511.3 m/z and no further fragmentation. Cpttt 2Sc is stable in solution at room temperature in alkane and aromatic solvents and in the solid state for at least several weeks. However, in Et₂O or THF, solutions of Cpttt2Sc decompose slowly over several days, marked by the loss of their red color. A 2.6 mM solution in THF was monitored by UV-visible spectroscopy over 83 h, and the decomposition was well modeled by first-order kinetics, yielding a rate constant $k = 2 \times 10^{-4} \text{ min}^{-1}$ and a half-life of ca. 2.5 days. This is in marked contrast to $Sc(P_2C_3^{t}Bu_3)_2$ which was reported to immediately decompose in THF.⁴

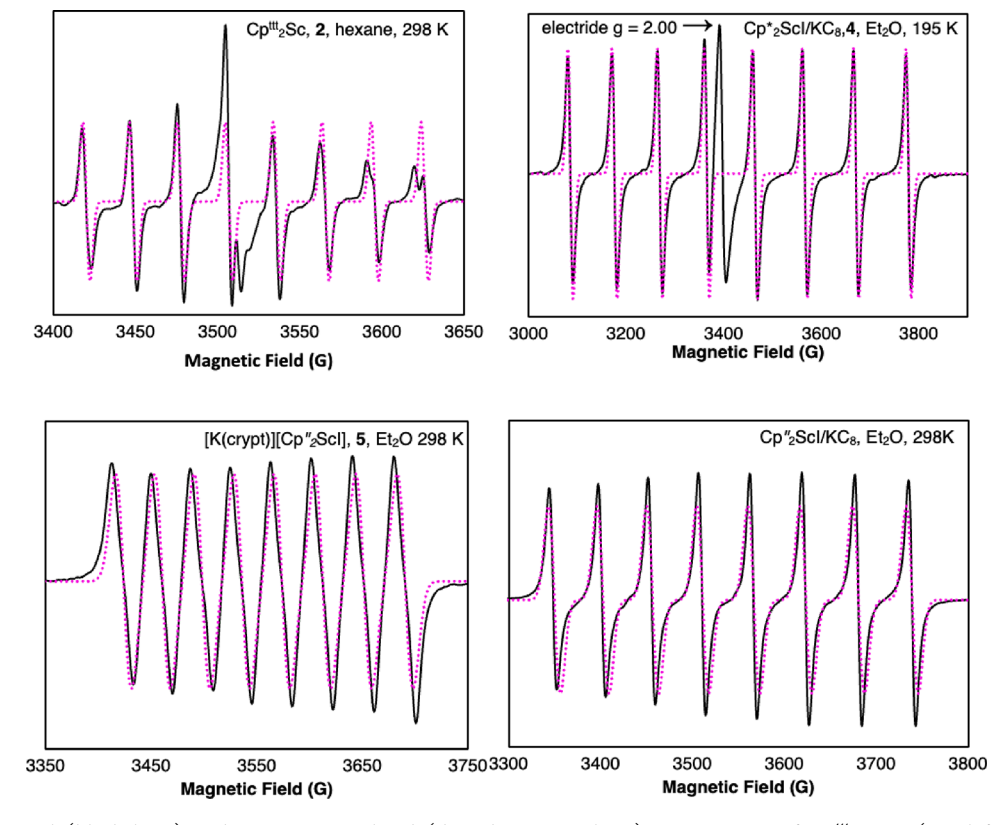


Figure 5. Experimental (black lines) and EasySpin-simulated (dotted magenta lines) EPR spectra of Cp^{ttt}_2Sc , 2 (top left), the Cp^*_2Sc/KC_8 reduction product, 4 (top right), $[K(crypt)][Cp''_2ScI]$, 5 (bottom left), and Cp''_2ScI/KC_8 reduction product formed in the absence of 2.2.2-cryptand (bottom right).

Table 1. EPR g Values and ⁴⁵Sc Hyperfine Coupling Constants of Reported Sc(II) Molecular Complexes

compound	$g_{\rm iso}$	$A_{ m iso}$	T (K)	ref
Cp ^{ttt} ₂ Sc, 2	1.99	82.6 MHz/29.6 G	298	this work
$Sc(P_2C_3tBu_3)_2$	1.98	103 MHz/37 G	120	4
K(crypt)][Cp" ₂ ScI], 5	1.98	105 MHz/37.9	298	this work
Cp" ₂ ScI/KC ₈	1.97	154 MHz/55.4 G	298	this work
	1.98	592 MHz/214 G	298	5
Cp* ₂ ScI/KC ₈ , 4	1.99	284 MHz/102 G	195	this work
$ \begin{array}{l} [\text{K(crypt)}[\text{Sc}(\text{OC}_6\text{H}_2\text{-}\\ \text{2,6-Bu}_2\text{-4-Me})_3] \end{array} $	2.01	819 MHz/291 G	77	6

Sc(II) with C_5Me_5 (Cp*). Formation of $Cp^*_2Sc(C_6H_5)$, 3. Given the successful isolation of Cp^{ttt}_2Sc by reduction of Cp^{ttt}_2ScI with KC_8 in hexane solvent (eq 4), the analogous reaction of $Cp^*_2ScI^{31,41}$ with KC_8 in hexane was examined. The initially yellow mixture became pale green over 1 week, but only unreacted Cp^*_2ScI was recovered from the mixture. The reduction in benzene was examined next since arenes were used successfully in the reduction of Cp^{iPr5}_2LnI complexes to form $Cp^{iPr5}_2Ln.^{11}$ In benzene, overnight stirring of a yellow mixture of Cp^*_2ScI and 2 equiv of KC_8 afforded an orange product. Recrystallization of this material from hexane afforded colorless crystals of $Cp^*_2Sc(C_6H_5)$, 41 3, in low yield (eq 5).

The ^{1}H NMR spectrum of 3 matches that reported in the literature for the same compound synthesized from $Cp*_{2}ScCl$ and phenyllithium. 41 Since the structure of $Cp*_{2}Sc(C_{6}H_{5})$ was

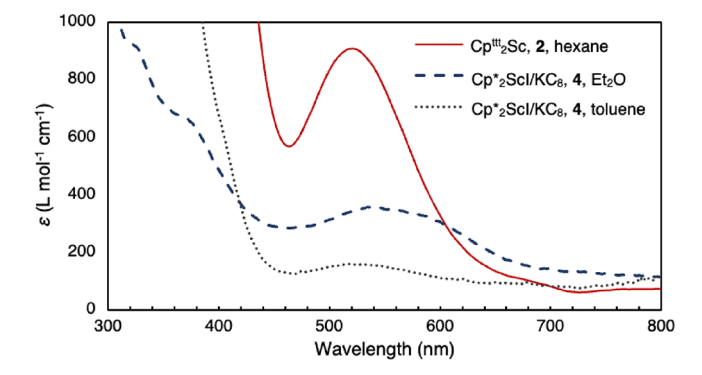


Figure 6. UV-visible spectra of Cp^{tt}₂Sc, 2, in hexanes at 298 K (red solid line), an Et₂O solution of the Cp*₂ScI/KC₈ reduction product, 4, at 195 K (dashed blue line), and a toluene solution of *in situ* generated 4 at 195 K (dotted gray line).

$$Cp*_{2}ScI + 2 KC_{8} \xrightarrow{\text{benzene, 25 °C}} Sc^{III}$$
(5)

not previously reported, complex 3 was definitively characterized by X-ray crystallography (Figure 7). Structural details are presented in the Supporting Information.

The progress of the reaction in eq 5 was followed in C_6D_6 by ¹H NMR spectroscopy. The Cp* resonance of Cp*₂ScI at 1.89 ppm disappeared over 2 days, and two new resonances were observed. One of these at 1.73 ppm was indicative of the

Figure 7. Molecular structure of $Cp*_2Sc(C_6H_5)$, 3, with thermal ellipsoids drawn at 30% probability and hydrogen atoms not shown for clarity. Selected bond distances (Å) and angles (°): $Sc-C_{Cp}$ (avg): 2.4760(1), Sc-Cnt1:2.163(1), Sc-Cnt2:2.161(1), Sc-C21:2.2495(1); Cnt1-Sc-Cnt2:143.23, Cnt1-Sc-C21:109.1, Cnt2-Sc-C21:107.7.

formation of Cp*2Sc(C6D5), while the second at 1.96 ppm has not been identified and is distinct from the 1.90 ppm resonance of $(Cp*_2ScH)_n$. Upon exchanging the solvent in this sample to C₆H₆, examination of the ²H NMR spectrum showed two triplets at 1.92 and 1.69 ppm, which were indicative of the presence of CH₂D methyl substituents that result from H-D exchange at the Cp* ligands of the two products formed in this reaction. Incorporation of deuterium into Cp* methyl groups is a phenomenon that has been previously described by Bercaw and co-workers for pentamethylcyclopentadienyl Sc(III) complexes in deuterated solvent.41 Additionally, a signal in the 2H NMR was observed at 7.59 ppm, which is in the region of the 7.3 ppm ¹H NMR resonance calculated by Bercaw and co-workers for the weighted average signal of the hydride in the oligomeric [Cp*2ScH]_n.⁴¹ The 7.59 ppm signal is significantly broadened $(\Delta \nu_{1/2} = 2.5 \text{ Hz})$ in comparison to the triplets at 1.69 and 1.92 ppm ($\Delta \nu_{1/2} = 0.5$ Hz), which is consistent with a hydride interacting with the I = 7/2 Sc nucleus. Thus, the 7.59 ppm signal could arise from a deuteride bound to scandium, formed by the C-H activation of deuterated benzene in the process that forms 3, although we have been unable to structurally authenticate this hydride species.

While the activation of C–H bonds by alkyl and hydrido scandium(III) complexes has been known for decades via σ bond metathesis, ⁴¹ the formation of 3 via eq 5 is unusual for scandium. Since several examples of C–H bond activation during Ln(III) to Ln(II) reduction reactions have been reported, ^{14,42–47} the formation of 3 in eq 5 suggested that the reduction of Cp*₂ScI may have formed a highly reactive Sc(II) species *in situ*. There is also precedent in titanium metallocene chemistry for C–H bond activation in reductions of Ti(III) complexes. ^{48,49}

 $Cp*_2Scl/KC_8$ **4.** Encouraged by this C–H bond activation result and data described in the next section on the reduction of Cp''_2ScI in diethyl ether, the reaction of 2 equiv of KC_8 with $Cp*_2ScI$ in diethyl ether at ca. -78 °C was conducted. This resulted in the immediate formation of an intensely dark-red solution of a new complex, **4**, similar in color to solutions of Cp^{tt}_2Sc , **2**. While the EPR spectrum of a frozen aliquot of the Et_2O solution of **4** at 77 K was complex and difficult to interpret due to apparent anisotropy, the spectrum in liquid solution at 195 K displayed an eight-line pattern characteristic of Sc(II) with $g_{iso} = 1.99$ and a hyperfine value of $A_{iso} = 284$ MHz (102 G) (Figure 5). Ambient temperature EPR data

could not be collected due to the thermal instability of this material; solutions of 4 decomposed within 1 min while warming to ambient temperature. In further support of the presence of Sc(II), the electronic spectrum of 4 (Figure 6), showed a low-intensity absorbance at 538 nm, which is very similar in energy to the 520 nm absorbance in the spectrum of Cp^{ttt}_2Sc , 2. Surprisingly, reduction of Cp^*_2ScI in *toluene* at -78 °C also gave a red-colored solution that has an EPR spectrum at 77 K and UV—visible spectrum (Figure 6), similar to that of 4 in Et₂O. The product of the reduction of Cp^*_2ScI in toluene was likewise thermally unstable.

The decomposition products of 4 in these solvents were examined by ¹H NMR spectroscopy. The residue from toluene solutions of 4 contained signals consistent with the formation of $Cp*_2Sc(CH_2C_6H_5)$ as well signals that most likely correspond to a mixture of the previously reported ortho-, meta-, and para-tolyl Cp*2Sc(C₆H₄CH₃) complexes.⁴¹ The crude material obtained from the reduction in Et₂O displayed a signal corresponding to unreacted Cp*2ScI along with signals, which suggested the formation of $Cp*_2Sc(OCH_2CH_3)$ and the previously reported Cp*2Sc(CH2CH3).50 These three signals appeared in an approximate 1:1:0.8 ratio. While some other minor signals were apparent in this spectrum, none could be attributed to known compounds. This, along with the unequal ratio of ethoxide to ethyl signals in the product mixture, highlights the highly reactive nature of complex 4 that forms upon reduction of Cp*₂ScI with KC₈.

Sc(II) with $C_5H_3(SiMe_3)_2$ (Cp''). [K(crypt)][Cp''_2ScI], 5. The reduction of Cp''_2ScI had previously been attempted by Lappert and co-workers using [$K(18\text{-crown-6})]_2[1,2,4,5\text{-}(SiMe_3)_4C_6H_2]$ as the reductant. However, the only product isolated from that reaction was the bridging reduced-ethylene complex, $Cp''_2Sc(\mu\text{-}CH_2CH_2)ScCp''_2$, in which the $(CH_2CH_2)^{2-}$ ligand was thought to arise from decomposition of 18-crown-6. Initially, the reduction of Cp''_2ScI in hexanes using KC_8 was examined in analogy to eq 4 with Cp^{ttt}_2ScI above. However, no reaction was observed after stirring at room temperature for 1 week. Similarly, no reaction was observed between Cp''_2ScI and KC_8 in benzene.

However, addition of a -35 °C solution of Cp″₂ScI in Et₂O to KC₈ precooled to -35 °C led to immediate formation of a green-brown mixture. Although we were unable to grow crystals suitable for X-ray diffraction from this solution, the EPR spectra at both 298 and 77 K contained eight-line patterns consistent with the presence of a Sc(II) ion. The 298 K EPR spectrum (Figure 5) had signals at $g_{\rm iso}=1.97$ with an $A_{\rm iso}=154$ MHz (55.4 G), and the 77 K EPR spectrum had an anisotropic eight-line pattern centered at g=1.98. The UV–visible spectrum of the green-brown solution was distinctly different from the spectra of red 2 and 4 and contained an absorbance at 430 nm (Figure 8).

When $\mathrm{Cp''}_2\mathrm{ScI}$ is reduced with $\mathrm{KC_8}$ in $\mathrm{Et_2O}$ at $-35\,^{\circ}\mathrm{C}$ in the presence of 2.2.2-cryptand (crypt), a green-brown solution also forms that has a UV-visible spectrum identical to that of the chelate-free reduction product just described with an absorbance maximum at 430 nm (Figure 8). The EPR spectrum at 298 K of this solution showed an eight-line pattern with g_{iso} of 1.98 and a coupling constant A_{iso} of 105 MHz (31.9 G). After filtering off the black solids (presumably graphite), dark-brown crystals suitable for single-crystal X-ray diffraction were grown after 1 h in a $-35\,^{\circ}\mathrm{C}$ freezer, which were identified as $[\mathrm{K}(\mathrm{crypt})][\mathrm{Cp''}_2\mathrm{ScI}]$, 5 (Figure 9, eq 6).

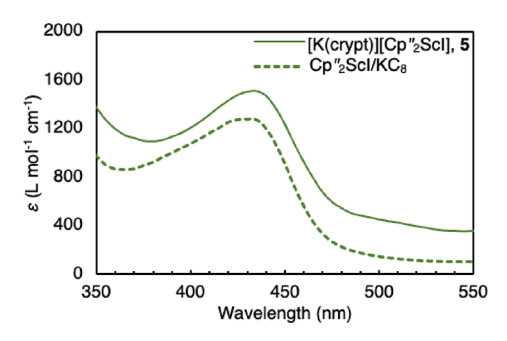


Figure 8. UV-visible spectra in Et₂O of [K(crypt)][Cp"₂ScI], 5 (solid line), and the reduction product of Cp" 2ScI and KC8 without 2.2.2-cryptand (dashed line).

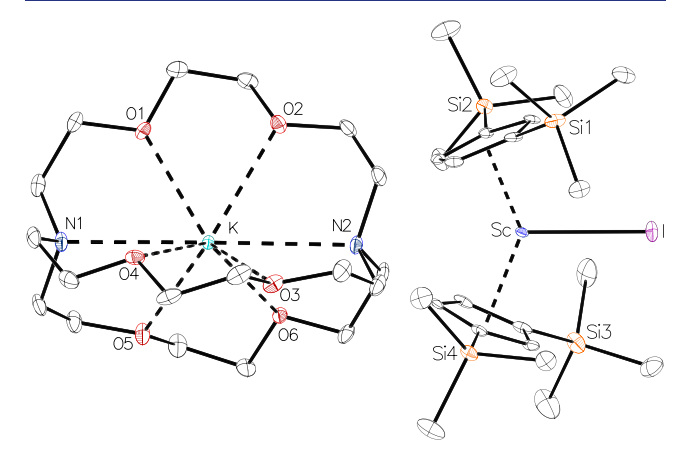
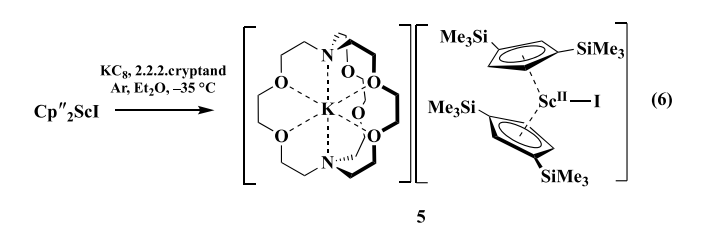


Figure 9. Molecular structure of [K(crypt)][Cp"₂ScI], 5, with ellipsoids at 50% probability with hydrogen atoms not shown and the cation and anion drawn separately for clarity.



The X-ray crystal structure of 5 revealed that with the Cp" ligand, a bis(cyclopentadienyl) Sc(II) complex is formed that retains an iodide ligand attached to the metal. The [Cp"₂ScI]¹⁻ anion is reminiscent of the $[Cp^{ttt}_2Ln(\mu-X)K(18\text{-crown-6})]$ complexes of Deacon et al., ¹⁴, ¹⁵ eq 3, except that the use of crypt results in a separated [K(crypt)]¹⁺ countercation.

Complex 5 has Sc-(Cp" ring centroid) distances of 2.184(1) Å and 2.200(1) Å that are only slightly longer than the 2.155(1) and 2.156(1) Å distances in Cp^{ttt}_2Sc , 2. The 139.9° (Cp" ring centroid)-Sc-(Cp" ring centroid) angle is much smaller than the 170.6° angle in Cpttt2Sc due to the presence of the iodide ligand. The 2.8902(6) Å Sc-I distance in 5 can be compared to the 2.8569(3) and 2.8194(3) Å Sc-I distances in Cp**2ScI, respectively.

In contrast to 2, even the crystalline material of [K(crypt)]-[Cp"ScI], 5 is thermally unstable, turning from dark red to light brown within hours at ambient temperature. Thermal decomposition of 5 in Et₂O was examined by monitoring the decay of the 430 nm absorbance in the UV-visible spectrum of a 9.2 mM solution. The data fit second-order kinetics with k= $12 \text{ M}^{-1}\text{min}^{-1}$ and a half-life of ca. 12 min.

Due to the thermal instability of 5, the magnetic susceptibility was determined by the Evans NMR method at low temperature on a sample of 5 generated in situ in d_8 -THF by the reaction of Cp"₂ScI, KC₈, and crypt. If it is assumed that quantitative conversion to 5 occurs and no decomposition occurs, a magnetic moment of 1.5 µB was calculated for [K(crypt)][Cp"2ScI], 5. This should be regarded as a lower limit given that the conversion is not likely to be quantitative and some decomposition is likely. Nevertheless, this is in agreement with what is expected for a Sc(II) ion with a 3d1 electron configuration.

Formation of $[Cp*_2Sc(18-Crown-6-\kappa^2O,O')][Cp*_2ScI_2]$, **6**. Given the success of generating [K(crypt)][Cp"₂ScI] according to eq 6, the reduction of Cp*2ScI was revisited in the presence of the chelates crypt and 18-crown-6 to potentially isolate a compound containing the [Cp*2ScI]1- anion. The reaction of a -78 °C diethyl ether solution of Cp*2ScI with 2 equiv of KC₈ in the presence of crypt afforded an intense blueviolet solution in contrast to the red solution described above for the chelate-free reaction. However, no Sc(II) complexes were isolated or detected spectroscopically. In contrast, when 18-crown-6 was used as the chelate under identical conditions, the yellow Cp*2ScI solution immediately became amber in color. Filtration of this mixture and concentration of the filtrate afforded a small amount of colorless crystals of the salt $[Cp*_2Sc(18\text{-crown-}6-\kappa^2O,O')][Cp*_2ScI_2]$, 6, which were characterized by X-ray diffraction (Figure 10, eq 7).

Formally, the reaction does not require any KC₈, since the net reaction is a ligand redistribution of iodide to make the

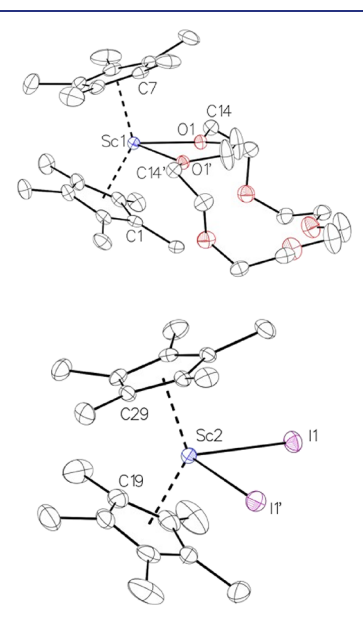
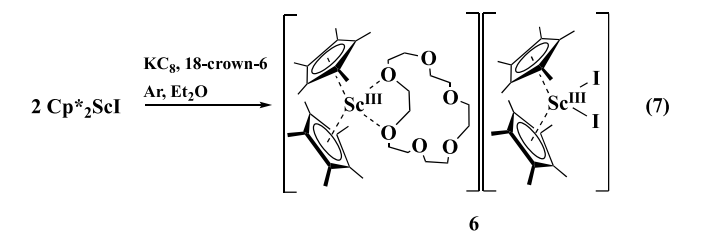


Figure 10. Molecular structure of $[Cp*_2Sc(18\text{-crown-}6-\kappa^2O,O')]$ -[Cp*2ScI2], 6, with thermal ellipsoids drawn at 30% probability. For clarity, the cation (top) and anion (bottom) have been drawn separately and hydrogen atoms and disorder associated with the crystallographic plane of symmetry are not shown. Selected distances (Å) and angles (°) where Cnt1 involves C1; Cnt2 involves C7; Cnt3 involves C21; Cnt4 involves C27: Sc1-C(Cp*)(avg), 2.510(2); Sc1-Cnt1, 2.204(3); Sc1-Cnt2, 2.217(3); Sc-O1, 2.259(3); Sc2-C(Cp*)(avg), 2.551(2); Sc2-Cnt3, 2.250(3); Sc2-Cnt4, 2.257(4); Sc2-I1, 2.9458(9); Cnt1-Sc1-Cnt2, 136.70(14); Cnt1-Sc1-O1, 107.88(11); Cnt2-Sc1-O1, 106.95(12); O1-Sc1-O1', 71.54(16); Cnt3-Sc2-Cnt4, 135.00(17); Cnt3-Sc2-I1, 105.28(7); Cnt4-Sc2-I1, 103.47(13); I1-Sc2-I1', 88.26(3).



 $[\mathrm{Cp}^*_2\mathrm{Sc}(18\text{-crown-6})]^{1+}$ cation and the $[\mathrm{Cp}^*_2\mathrm{ScI}_2]^{1-}$ anion. However, complex **6** was not formed by treating $\mathrm{Cp}^*_2\mathrm{ScI}$ with 18-crown-6 in the absence of KC_8 and neither $\mathrm{Cp''}_2\mathrm{ScI}$ nor $\mathrm{Cp''}_2\mathrm{ScI}$ was observed to react this way with KC_8 in the presence of 18-crown-6. The structure of **6** is further described in the Supporting Information.

Computational Analysis. Electronic structure calculations were performed on Cp^{ttt}₂Sc, Cp*₂Sc, Cp"₂Sc, and (Cp"₂ScI)¹⁻ using density functional theory (DFT) with the TPSSh hybrid meta-generalized gradient density functional^{51,52} including Grimme's D3 dispersion correction⁵³ with the Becke–Johnson damping function.⁵⁴ The double- ζ quality split-valence basis sets with polarization functions def2-SV(P)⁵⁵ were used for nonmetallic atoms. Triple-zeta quality basis sets def2-TZVP^{56,57} were used for Sc. The solvation effects were taken into account by using the COSMO model⁵⁸ with a dielectric constant of 1.887 and an index of refraction of 1.3727 for hexane. The electronic spectra were simulated using timedependent density functional theory (TDDFT) computations. All calculations were performed with the TURBOMOLE quantum chemistry package (developer version)⁵⁹ using DFT methods applicable to organometallic rare-earth metal compounds. 60 Complete details can be found in the Supporting Information. The structural predictions and predicted hyperfine coupling constants from the calculations are shown in Table 2, and natural population analysis (NPA) calculations are given in the Supporting Information.

Table 2. Calculated Structural Parameters and Hyperfine Constants for Cp^{ttt}₂Sc, Cp*₂Sc, Cp"₂Sc, and (Cp"₂ScI)¹⁻ Compared with Experimental Values for Cp^{ttt}₂Sc, 2, and [K(crypt)][Cp"₂ScI], 5

complex	Sc-(ring centroid) distance (Å)	(ring centroid)- Sc-(ring centroid) angle (°)	calculated electron configuration	hyperfine coupling constant (A, MHz)
Cp ^{ttt} ₂ Sc (calc)	2.14	168.4	$3d^1$	82.5
Cp ^{ttt} ₂ Sc, 2 (exp)	2.155(1), 2.156(1)	170.6		82.6
Cp*2Sc (calc)	2.09	163.0	$3d^1$	103.8
Cp" ₂ Sc (calc)	2.10	146.9	$3d^1$	53.2
(Cp" ₂ ScI) ¹⁻ (calc)	2.16	135.1	$3d^1$	105.3
(Cp" ₂ ScI) ¹⁻ , 5 (exp)	2.184(1), 2.200(1)	139.9		105.4

As shown in Table 2, the DFT-optimized structure of Cp^{ttt}₂Sc, calculated on the basis of the X-ray crystal data on 2, had a Sc-(Cp^{ttt} ring centroid) distance and a (Cp^{ttt} ring centroid)-Sc-(Cp^{ttt} ring centroid) angle very close to the values found in the solid-state structure at 93 K. The calculated structural parameters were similar with and without Grimme's D3 dispersion correction and are reported in the Supporting Information. The NPA calculations are consistent with a Sc(II)

center with a $3d^1$ electronic configuration. The HOMO and LUMO are shown in Figure 11. The HOMO derives from a d_{xy} or $d_{x^2-y^2}$ orbital using the conventional assignment of Cartesian coordinates for bent metallocenes.⁵⁸

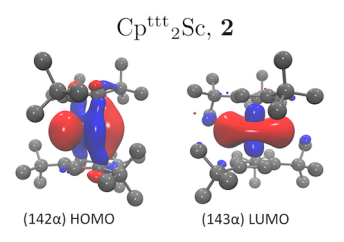


Figure 11. Frontier molecular orbital plots for Cp^{ttt}₂Sc, **2.** Hydrogen atoms are not shown for clarity. A contour value of 0.03 was used to depict the orbitals.

The calculations match the slightly bent structure observed in the crystal structure of **2**. The bending can be explained by a first-order Jahn—Teller effect using the bent metallocene Walsh diagrams published in 1976 by Lauher and Hoffmann. The doubly degenerate ground state for a linear d¹ Cp^{ttt}₂Sc will split with single occupancy to give a more stable bent structure.

TDDFT calculations carried out to analyze the electronic spectrum of 2 showed three sets of expected transitions that match well the observed spectrum, which contains an absorbance in the visible region at 520 nm as well as two high-intensity absorbances in the UV region at 286 and 394 nm (Figure 12). The DFT calculations also allowed a

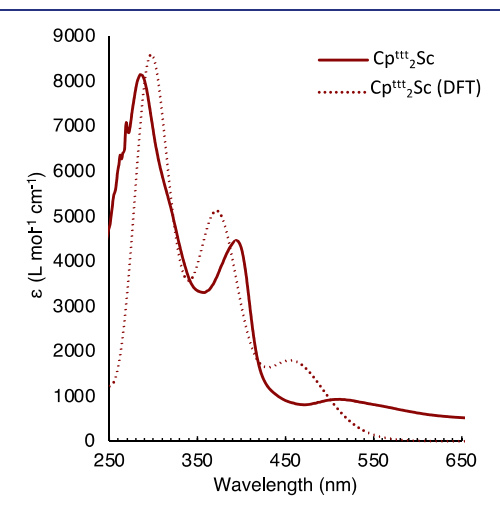


Figure 12. UV-Visible spectra of Cpttt₂Sc, 2, in hexanes (solid line) and computed (dotted line).

prediction of the EPR spectrum, and a hyperfine A value of 82.5 MHz was calculated, which matched the experimental value 82.6 MHz (29.6 G). Overall, there is excellent agreement between experiment and theory for $\operatorname{Cp^{tt}}_2\operatorname{Sc}$.

The DFT calculations also converge for a bent structure for Cp*₂Sc with a 163° (ring centroid)-Sc-(ring centroid) angle slightly less than that in Cp^{ttt}₂Sc, but shorter Sc-ring centroid distances of 2.09 Å compared to the 2.14 Å predicted for 2. The TDDFT prediction of the UV-visible spectrum of Cp*₂Sc matched that found for the red solution, 4, as shown in Figure 13. The hyperfine coupling constant calculated for Cp*₂Sc, 104 MHz, was larger than the 82.5 MHz predicted for Cp^{ttt}₂Sc, 2. This is consistent with previous studies of Y(II)

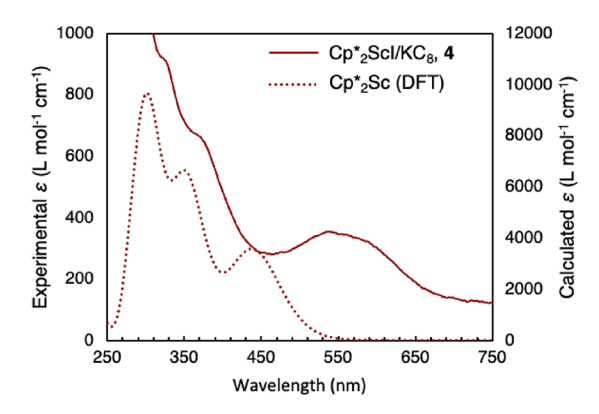


Figure 13. UV-visible spectra of the reaction between Cp^*_2ScI and KC_8 , 4, in Et_2O at 195 K (solid line) and computed (dotted line).

complexes of formula $[(C_5R_5)_3Y]^{1-}$ that showed a correlation of A values with electron donor strength of the ligands. Specifically, the $[(C_5R_5)_3Y]^{1-}$ complexes had A values, going from the least electron-donating to the more electron-donating C₅R₅ ligands as follows: Cp" 101 MHz (36.1 G); C₅H₄SiMe₃, 102 MHz (36.6 G), C₅H₅, 19.2 MHz (42.8 G); C₅H₄Me, 131 MHz (46.9 G). 42,62 The monodentate amide and aryloxide Y(II) analogues have much higher values: $\{Y[N(SiMe_3)_2]_3\}^{1-1}$ 304 MHz (110 G),⁶³ and $[Y(OAr^*)_3]^{1-}$, 425 MHz (153.3 G) (OAr* = OC₆H₂-2,6-Ad₂-4-^tBu).⁶⁴ Thus, while the calculated hyperfine coupling constant of 104 MHz for Cp*2Sc was consistent with its more electron-donating ligand environment in comparison to that of Cpttt2Sc, 2, the experimentally observed value of 284 MHz for the red solution, 4, constituted a large discrepancy between the calculated and observed value. In the absence of structural data on the Sc(II) containing species in 4, this discrepancy is not understood.

The DFT calculations on Cp"2Sc predicted an Sc-(ring centroid) distance similar to that of Cp*2Sc but with a significantly more bent structure with a 147° (ring centroid)-Sc-(ring centroid) angle. The predicted UV-visible spectrum was similar to that of Cp^{ttt}₂Sc and Cp*₂Sc. However, reduction of Cp"2ScI did not give this neutral Cp"2Sc product but rather the anionic $(Cp''_2ScI)^{1-}$ with an extra iodide ligand. With crystallographic data on [K(crypt)][Cp"₂ScI], 5, in hand as a starting point, calculations were done on the (Cp"2ScI)1anion. Like the calculations on Cpttt 2Sc, the calculations on (Cp"₂ScI)¹⁻ matched the structure obtained at 93 K quite well both in Sc-(ring centroid) and Sc-I distances and in the (ring centroid)-Sc-(ring centroid) angle (Table 2). In addition, the predicted EPR hyperfine coupling constant of 105 MHz exactly matched the observed for 5. This value is larger than that of 2 in contrast to the observed trend in $[(C_5R_5)_3Y]^{1-}$ complexes. However, the comparison of A values for Cpttt 2Sc and [K(crypt)][Cp"₂ScI] is not so straightforward since the two compounds have a different number of ligands. Although Cpttt is more electron-donating than Cp", the relative effect of the inclusion of the iodide ligand in [K(crypt)][Cp"2ScI] is unknown. The TDDFT prediction of the UV-visible spectrum differed from those of red Cpttt2Sc, Cp*2Sc, and Cp"2Sc and matched well the observed spectrum of green-brown 5 (Figure 14).

Guzei Analysis. One of the crucial factors in isolating highly reducing low oxidation state rare-earth metal complexes appears to be steric saturation of the coordination environment. One method to evaluate the steric saturation around a

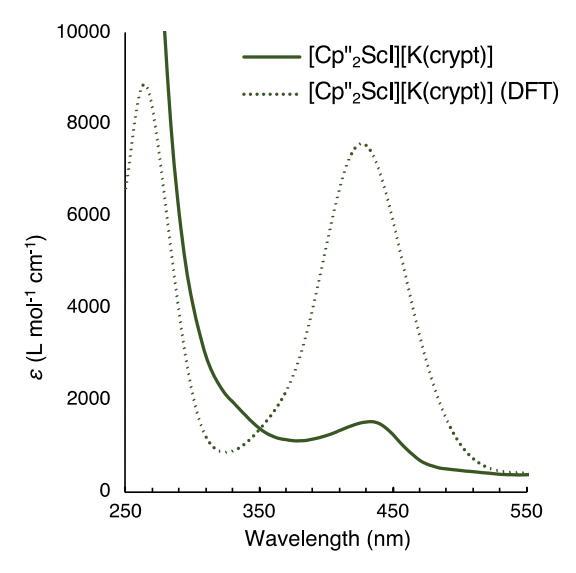


Figure 14. UV-visible spectra of [K(crypt)][Cp"₂ScI], 5, in Et₂O (solid line) and calculated (dotted line).

metal center involves calculation of the Guzei solid angle, G, that provides an estimation of the percentage of the coordination sphere of the metal that is protected by the ligands. Guzei G values for low oxidation state rare-earth metal and actinide complexes that form isolable crystallographically characterizable compounds are typically over 80%. This metric is not absolute; however, it is generally best to compare G values only for a structurally similar series of complexes. 64,68,69

The G values of $\operatorname{Cp^{ttt}}_2\operatorname{Sc}$, 2, and $[K(\operatorname{crypt})][\operatorname{Cp''}_2\operatorname{ScI}]$, 5, were calculated based on the X-ray crystal structures while G values for $\operatorname{Cp''}_2\operatorname{Sc}$ and $\operatorname{Cp''}_2\operatorname{Sc}$ were estimated based on DFT-generated structures (Table 3). It should be noted that G

Table 3. Solid G Values for Selected Crystallographically Characterized or DFT-Generated Compounds

compound	G value
$Cp^{ttt}{}_{2}Sc$ (exp)	87%
Cp* ₂ Sc (calc)	75%
Cp″ ₂ Sc (calc)	89%
$[\mathrm{Cp''}_2\mathrm{ScI}]^{1-}\ (\mathrm{exp})$	88%
Cp ^{iPr5} ₂ La (exp)	89%
Cp ^{iPr5} ₂ Lu (exp)	90%

values generated from DFT calculations may differ from values obtained from X-ray crystal data. For example, a G of 93% was found from a DFT-generated structure for $(C_5H_4Si^iPr_3)_3Th$, but when subsequent X-ray data were obtained, the G was 88%. The difference could arise from packing effects in the solid state that cannot be taken into account in gas-phase DFT calculations. A further caveat on DFT-generated G values from that study is that $(C_5H_4Si^iPr_3)_3Th$ and " $(C_5H_4SiMe_3)_3Th$ " have similar Guzei values, 89% (from X-ray) and 87% (from DFT), respectively, yet $(C_5H_4Si^iPr_3)_3Th$ is a room-temperature stable compound that can be crystallographically analyzed and " $(C_5H_4SiMe_3)_3Th$ " is too reactive to even isolate at low temperature.

The crystallographically generated G values of 87% for Cp^{ttt}_2Sc and 88% for $[K(crypt)][Cp''_2ScI]$, **5**, are in the high range expected for stable complexes. The DFT-generated G of

75% for $\operatorname{Cp*}_2\operatorname{Sc}$ is consistent with the fact that this complex was not isolated. It was surprising, however, to find that the G value for DFT-generated $\operatorname{Cp''}_2\operatorname{Sc}$ was 89%. It was expected that this value would be low and the isolation of 5 was possible because of the additional steric saturation provided by the iodide ligand bound to scandium. Likewise, the formation of $(\operatorname{Cp*}_2\operatorname{ScI})^{1-}$ seemed possible and that this would have appropriate steric saturation needed for its isolation. Clearly more experimental data are needed to evaluate these Guzei analyses.

DISCUSSION

Considering that the previously reported Sc(II) complexes like $Sc(P_2C_3^tBu_3)_2^5$ and $\{Sc[N(SiMe_3)_2]_3\}^{1-6}$ readily decompose at room temperature, it is remarkable that Cp^{ttt}_2Sc can be sublimed at 200 °C, melts at 268–271 °C without decomposition, and is stable for weeks in alkane and aromatic solvents at room temperature. Clearly, the steric and electronic factors involved in this specific bis(cyclopentadienyl) ligand environment are very favorable for stabilizing Sc(II).

As scandium occupies a unique place in the periodic table as the first member of the transition metals and the lightest member of the rare-earth metals (Sc, Y, and the lanthanides), the structure of 2 can be compared from two perspectives. First-row transition metal metallocenes $Cp^{R}_{2}M$ (Cp^{R} = cyclopentadienyl ligand; M = Ti - Ni, Zn) are generally "linear", i.e., the cyclopentadienyl ligands are parallel with most Cp^{R} groups. ^{29,30,70} However, other reported $Cp^{ttt}_{2}M$ complexes (M = Cr, Mn, Fe, Co)^{71–74} are bent, which has been attributed to steric effects of the ligands. 73,75 Direct comparisons with the closest transition metal, Ti, are complicated by C-H bond activation issues. 48,76,77 For the rare-earth metallocenes $Cp_{2}^{R}Ln$ (Ln = Y, La – Lu), both bent and linear structures are observed depending on the size of the cyclopentadienyl ligand. 9-11,16,18,78-81 In the case of d¹ Sc(II), the bending can be explained by a first-order Jahn-Teller effect arising from the singly occupied doubly degenerate d(xy), $d(x^2-y^2)$ HOMO in the case of a linear metallocene.⁶¹

The high thermal stability of **2** is reminiscent of the stability of the Cp^{iPrS}₂Ln complexes, which can be recrystallized from boiling hexane. Both can also be made by reduction of bis(cyclopentadienyl) iodide complexes in nonpolar solvents (hexane or benzene), a route that was also successful to isolate Cp^{ttt}₂Tm. The Cp^{iPrS}₂Ln complexes are, however, rigorously linear with the metal lying on an inversion center, in contrast even to the known Cp^{ttt}₂Ln complexes (Ln = Sm, Eu, Tm, Yb), 9,16,18 which are bent.

Although the -78 °C reductions of the pentamethylcyclopentadienyl analogue, Cp*2ScI, in Et2O or toluene gives a product with a UV-visible spectrum similar to that of Cpttt 2Sc and an eight-line EPR spectrum consistent with formation of a Sc(II) species, the analogous complex Cp*2Sc was not isolated due to the high instability of the reduction product even at low temperatures. Rather, C-H bond activation products from the Cp*2ScI/KC8 reduction reaction in aromatic solvents were identified by ¹H NMR spectroscopy and by X-ray crystallography in the case of $Cp_2^*Sc(C_6H_5)$, 3. No Sc(II) species were directly observed in these benzene reductions, likely due to the 5 °C freezing point of benzene precluding low-temperature investigations. Likewise, the ambient temperature reduction in Et₂O generates Cp*₂ScEt and a product with apparent ethoxide ¹H NMR resonances indicative of C-O cleavage of the solvent. From these findings, it is clear that if Cp*2Sc is

formed, it has available decomposition pathways that make it much less stable than Cp^{ttt}_2Sc .

On the other hand, reduction of Cp''_2ScI with KC_8 , like the Cp^{ttt}_2ScI system, gives an isolable, crystallographically characterizable Sc(II) product, $[K(crypt)][Cp''_2ScI]$, 5, reminiscent of the $[Cp^{ttt}Ln(\mu-X)K(18\text{-crown-6})]$ complexes of the larger rare-earth metals, Nd and Dy (eq 3). Given the smaller size of Cp'' compared to Cp^{ttt} , it makes sense that coordination of an extra ligand could give steric saturation comparable to Cp^{ttt}_2Sc .

Indeed, the 87% Guzei solid angle for $[K(crypt)][Cp''_2ScI]$, 5, matches the 88% G of Cp^{ttt}_2Sc . These values are in the range expected for sterically stabilized complexes and are near the G values for the Cp^{iPr5}_2Ln complexes, 10,11 which range from 89% for La to 90% for Lu (Table 3). However, it should be noted that despite the similar G values of 2 and 5, complex 5 is much less stable and 50% decomposition is observed in 10 min at room temperature in Et_2O compared to a 2.5 day half-life for 2 in THF. The presence of an iodide ligand in 5 that can be dissociated leading to a presumably less sterically hindered and more reactive Cp''_2Sc is a big difference from Cp^{ttt}_2Sc .

DFT calculations match well the experimental structural and spectroscopic properties of $Cp^{ttt}{}_2Sc$, 2, and $[K(crypt)]-[Cp''{}_2ScI]$, 5, and indicate a $3d^1$ electron configuration for each Sc(II) center. Comparison of the DFT calculations with experimental data is less clear for the red Cp*2ScI reduction product, 4, since no crystallographic data are available. The DFT calculations predict well the spectrum of the red solution based on a Cp*2Sc structure, but the predicted 104 MHz hyperfine coupling A value is not close to the 284 MHz value observed in the EPR spectrum of the red solution, 4. Comparison of the 104 MHz prediction for Cp*2Sc with the 82.6 MHz observed for Cpttt2Sc fits well with the trend of $[(C_5R_5)_3Y]^{1-}$ compounds since Cp* has more alkyl groups than Cpttt and would be expected to have a higher A value. Hence, if the hyperfine coupling constant calculations are good estimates, then the red solution must contain a Sc(II) complex other than Cp*2Sc. However, there is no doubt that a Cp*ligated Sc(II) complex exists and is highly reactive since it can generate Cp*2Sc(C₆H₅) from benzene and Cp*2ScEt from diethyl ether. The large hyperfine coupling constant suggests that the species has an electron configuration that allows strong interaction between the unpaired electron and the Sc nucleus.

The Cp*₂ScI reduction system is further unusual in that attempts to do the reduction with KC₈ in the presence of 18-crown-6 generate the salt, $[Cp*_2Sc(18\text{-crown-}6-\kappa^2O,O')]$ - $[Cp*_2ScI_2]$, **6**. This complex is just a simple ligand redistribution product from $Cp*_2ScI$ and 18-crown-6, yet it only forms in the presence of KC₈, which is not needed stoichiometrically.

CONCLUSIONS

ı

In conclusion, a thermally stable, crystallographically characterizable bis(cyclopentadienyl) complex of Sc(II) was shown to be obtainable by reduction of a bis(cyclopentadienyl) scandium iodide if the proper substitution on the cyclopentadienyl ring is present. Specifically, the tri-tert-butyl cyclopentadienide ligand, Cptt, provides the appropriate steric and electronic environment to stabilize the Sc(II) ion in Cptt_2Sc. This result finally extends the long known and extensively studied bis(cyclopentadienyl) chemistry of the transition metals to the first element in the transition metal series and the smallest metal of the rare-earth metal series.

Although reduction of Cp*2ScI gives solutions with spectroscopic properties similar to that of Cpttt 2Sc, the solutions are not thermally stable and the putative decamethylscandocene, Cp*2Sc, was not isolated. Instead, C-H and C-O bond activations of aromatic and ethereal solvents were observed. With the smaller bis(trimethylsilyl)cyclopentadienyl ligand, Cp", reduction of Cp"ScI can be achieved in Et₂O to form the Sc(II) salt $[K(crypt)][Cp''_2ScI]$, which defines another new class of Sc(II) species. The fact that Cpttt₂Sc can be sublimed at 200 °C suggests that there is nothing inherently unstable with bis(cyclopentadienyl)Sc(II) complexes, and it is likely that others can be synthesized. Although other Sc(II) complexes should be accessible, it is also true based on the formation of $Cp_2^*Sc(C_6H_5)$ from attempts to isolate Cp*2Sc that Sc(II) metallocenes should also be a source of high reactivity in the chemistry of this earliest member of the transition metal series.

■ EXPERIMENTAL SECTION

General Considerations. All manipulations were performed by using modified Schlenk techniques or in a Vacuum/Atmospheres glovebox under argon. Solvents were degassed by sparging with dry argon before drying and collection using an S2 Grubbs-type solvent purification system (JC Meyer).⁸² All physical measurements were recorded under strictly anaerobic and anhydrous conditions. Infrared spectra were recorded on compressed solid samples using an Agilent Cary 630 ATR/FTIR instrument. Electronic spectra were recorded as dilute solutions in the indicated solvent in quartz cuvettes (1 mm or 1 cm path length) using an Agilent Cary 60 UV/vis spectrophotometer. ¹H, ²H, and ¹³C{¹H} NMR spectra were recorded using a Bruker Avance 600 or 500 MHz spectrometer and referenced to residual solvent signals. X-band EPR spectra were recorded at the indicated temperature using a Bruker EMX spectrometer equipped with an ER041Xg microwave bridge and calibrated with DPPH (g = 2.0036). Magnetic moments were determined by Evans' method and corrected using the appropriate diamagnetic constants. 34-36 CHN analysis was performed at the UC Berkeley Microanalytical Facility. Scandium metal content was determined by complexometric titration of hydrolyzed samples with Na₂EDTA solution using xylenol orange as an indicator. 83–85 Scandium iodide was prepared from scandium metal and ammonium iodide in a modification of the procedure described by Meyer et al. ⁸⁶ KCp^{*tt} was prepared according to the literature procedure. ⁸⁷ Cp*₂ScI^{31,41} and Cp″₂ScI⁴² were prepared from the reaction of KCp* or KCp″ with ScI₃ in toluene analogously to 1 below and identified by their ¹H NMR spectra.

MALDI-TOF Mass Spectrometry. Mass spectra were recorded with an AB Sciex 5800 MALDI-TOF mass spectrometer in reflector mode using an anthracene matrix on a stainless-steel target plate. A saturated solution of anthracene in benzene and benzene solutions of 1 and 2 (ca. 10 mg in 1 mL) were used as targets. Inside an argonfilled glovebox, 1 μ L aliquots of the anthracene solution were spotted on the target plate and allowed to dry. Then, 1 μ L aliquots of the analyte solutions were added on top of the matrix and allowed to dry. A second 1 μ L aliquot of matrix solution was added and allowed to dry on top of each spot. The target plate was mounted on the plate holder inside of the glovebox, placed inside of a plastic box with an airtight lid, and removed from the glovebox. The target plate was quickly removed from the plastic box and loaded into the mass spectrometer's vacuum chamber. After the acquisition, the yellow spots of 1 and the red spots of 2 on the retrieved target plate were still strongly colored before removal from the spectrometer's vacuum

 $\mathsf{Cp^{ttt}}_2\mathsf{Scl}$, 1. Under an argon atmosphere, a pale yellow slurry of ScI_3 (213 mg, 0.50 mmol) and $\mathsf{KCp^{ttt}}$ (272 mg, 1.00 mmol) in ca. 20 mL of toluene was heated to ca. 110 °C for 3 days. The solvent was removed under vacuum and the residue extracted three times with ca. 15 mL of n-hexane. After separation of the solids by centrifugation

and filtration through a pipet packed with ca. 1 cm of Kimwipes, the combined bright-yellow supernatants were slowly evaporated under reduced pressure, yielding bright-yellow crystals of 1 (110 mg, 34%). X-ray quality crystals were grown by storage of a solution of ca. 0.100 g in 3 mL of toluene at -35 °C for 2 days. ¹H NMR (600 MHz, C_6D_6 , 298 K): δ = 7.84 (s, 2H, CpH), 7.09 (s, 2H, CpH), 1.57 (s, br, 18H, $-C(CH_3)_3$, 1.51 (s, br, 18H, $-C(CH_3)_3$, 1.10 (s, 18H, $-C(CH_3)_3$. $^{13}C\{^1H\}$ NMR (151 MHz, C_6D_6 , 298 K): δ = 142.52 (C^tBu), 141.57 (C^tBu), 140.23(C = C^tBu), 127.52 (C = CH), 112.84 (C = CH), 36.03 $(-C(CH_3)_3)$, 35.14 $(-C(CH_3)_3)$, 34.44 $(-C-C(CH_3)_3)$ $(CH_3)_3$), 33.92 $(-C(CH_3)_3)$, 33.53 $(-C(CH_3)_3)$, 31.62 $(-C(CH_3)_3)$ $(CH_3)_3$). ATR-FTIR (cm^{-1}) : 2956 (st), 2903 (m), 2868 (m), 1481(w), 1457(m), 1360 (st, sh), 1238 (m), 1204(m), 1168 (m), 1110 (w), 996 (w), 955 (w), 919 (w), 848 (st, sh), 800 (m), 680 (m), 663 (m). M.P. > 260 °C, no decomposition up to this temperature. UV-vis (n-hexane, 298 K), $\lambda_{\text{max}}/\text{nm}(\varepsilon/\text{M}^{-1}\text{cm}^{-1})$: 371 (ε = 2000). Anal. Calcd for ScC₃₄H₅₈I: Sc 7.0; found: Sc 6.9. MALDI-TOF MS, positive ion mode, m/z: 405.0 ([Cp^{ttt}ScI]⁺), 456.2 ([Cp^{ttt}Sc-(anthracene)]⁺), 511.3 ([Cp^{ttt}₂Sc]⁺). Negative ion mode, m/z: 126.9 ([I]⁻), 233.2 ([Cp^{ttt}]⁻), 425.6 ([ScI₃]⁻), 476.8 ([ScI₂(anthracene)]⁻), 532.0 ([Cp^{ttt}ScI₂]⁻).

Cpttt2Sc, 2. In an argon-filled glovebox free of volatile Lewis bases, a mixture of Cpttt₂ScI (65 mg, 0.10 mmol) and KC₈ (15 mg, 0.11 mmol) in ca. 8 mL of n-hexane was stirred for 6 days, during which time the color changed from yellow to dark red. The solids, presumably graphite and KI, were separated by centrifugation and subsequent filtration through a pipet packed with 1 cm of Kimwipes. Removal of the solvent under reduced pressure yielded Cptt 2Sc, 2, as a dark-red powder, which was sublimed at 200 °C and 10⁻⁴ Torr (39 mg, 75%). Slow evaporation at ambient temperature of a ca. 0.25 mL aliquot of an *n*-hexane solution of Cp^{ttt}₂Sc in a 20 mL scintillation vial inside the glovebox overnight gave several red needles of 2 suitable for X-ray diffraction. 1H NMR (600 MHz, C_6D_6 , 298 K): δ = 0.30 (br, 36H, $-C(CH_3)_3$, -0.10 (br, 18H, $-C(CH_3)_3$). ATR-FTIR (cm⁻¹): 2952 (st), 2900 (m), 2864 (m), 1477 (m), 1455 (m), 1385 (m), 1357 (st, sh), 1236 (st, sh), 1199 (w), 1154 (w), 1107 (w), 1021 (w), 998 (w), 956 (w), 920 (w), 803 (st), 723 (w), 684 (m), 671 (w). M.P. 268–271 °C. UV–vis (*n*-hexane, 298 K) $\lambda_{\rm max}$ /nm (ε /M⁻¹cm⁻¹): 286 $(\varepsilon = 14000)$, 394 $(\varepsilon = 7500)$, 520 $(\varepsilon = 900)$. Magnetic moment (Evans' method, benzene): 1.9 μ_B . Anal. Calcd for ScC₃₄H₅₈: C 79.8, H 11.4, Sc 8.8; Found: C 79.7, H 11.4, Sc 8.6. MALDI-TOF MS m/z: 511.3 ([Cp^{ttt}₂Sc]⁺).

 $\mathsf{Cp*}_2\mathsf{Sc}(\mathsf{C}_6\mathsf{H}_5)$, **3.** In an argon-filled glovebox free of volatile Lewis bases, $\mathsf{Cp*}_2\mathsf{ScI}$ (0.10 g, 0.23 mmol) was dissolved in ca. 10 mL of benzene. KC_8 (0.062 g, 0.46 mmol) was then added to this yellow solution in one portion. After stirring for 18 h, the mixture became orange in color. The solvent was removed under reduced pressure, and the residue was extracted in ca. 10 mL of hexane. The mixture was centrifuged, and the supernatant was filtered. The filtrate was concentrated to ca. 1 mL volume by removal of the solvent under reduced pressure. Overnight storage of this orange solution afforded a small amount of colorless crystals of $\mathsf{Cp*}_2\mathsf{Sc}(\mathsf{C}_6\mathsf{H}_5)$, **3.** This reaction was studied in more detail by NMR spectroscopy (vide infra).

Reduction of Cp*₂ScI with KC₈ in Diethyl Ether, Cp*₂ScI/KC₈, 4. In an argon-filled glovebox, a solution of Cp*₂ScI (0.10 g, 0.23 mmol) in ca. 4 mL of diethyl ether was cooled to ca. -78 °C in a 20 mL vial. KC₈ (0.031 g, 0.23 mmol) was then added to the solution in one portion. The mixture immediately became dark red and was gently swirled for ca. 20 s. The EPR spectra of aliquots of this solution at 77 and 195 K showed eight-line resonances consistent with the formation of Sc(II). UV—vis (Et₂O, 195 K) λ_{max} /nm (ε /M⁻¹cm⁻¹): 535 (300).

In another reaction, $\mathrm{Cp*_2ScI}$ (0.025 g, 0.056 mmol) was dissolved in ca. 5 mL of diethyl ether in a 20 mL vial and the solution was cooled to ca. -78 °C. $\mathrm{KC_8}$ (0.008 g, 0.06 mmol) was added to the solution in one portion. The mixture immediately became dark red in color and was allowed to stand at this temperature for 18 h. After the mixture was allowed to warm to ambient temperature and stirred for 1 h, the solution was decanted from the black solids, presumably graphite, at the bottom of the vial, and the solvent was removed from

this solution under reduced pressure to give a yellow residue. This crude residue was then dissolved in C_6D_6 for study by 1H NMR spectroscopy, which showed resonances consistent with the presence of $Cp^*_2ScI,^{41}$ $Cp^*_2ScCH_2CH_3,^{50}$ and a third complex that we have tentatively assigned as $Cp^*_2ScOCH_2CH_3$. 1H NMR (500 MHz, C_6D_6): δ = 4.49 (q, 2H, OC H_2 CH $_3$ (Cp^*_2ScOEt), J_{HH} = 6.9 Hz), 1.93 (s, 30H, CH $_3$ ($Cp^*_2ScOCH_2CH_3$)), 1.91 (s, 30H, CH $_3$ (Cp^*_2ScI)), 1.86 (s, 30H, CH $_3$ ($Cp^*_2ScCH_2CH_3$), 1.33 (t, 3H, CH $_3$ ($Cp^*_2ScCH_2CH_3$), J_{HH} = 6.9 Hz), 0.99 (q, 2H, CH $_3$ ($Cp^*_2ScCH_2CH_3$), J_{HH} = 8.2 Hz), 0.17 (t, 3H, CH $_3$ ($Cp^*_2ScCH_2CH_3$), J_{HH} = 8.2 Hz).

NMR Scale Reduction of Cp*₂ScI with KC₈ in Benzene-D₆. Cp*₂ScI (0.010 g, 0.020 mmol) and KC₈ (0.003 g, 0.02 mmol) were combined in a J. Young NMR tube, and ca. 0.5 mL of deuterated benzene was added. The tube was sealed, and the mixture was briefly shaken. The reaction mixture was periodically monitored by ¹H NMR spectroscopy, which indicated that the Cp*2ScI was completely consumed after 2 days. The spectrum showed that the reaction formed Cp*2Sc(C5D5) and a second product containing a Cp* ligand. ¹H NMR of mixture (500 MHz, C_6D_6 , 2 day reaction time): $\delta = 1.96$ (s, CH₃ (Cp*), Cp* containing product), 1.89 (s, CH₃ (Cp*), residual Cp*₂ScI), 1.73 (s, CH₃ (Cp*), Cp*₂Sc(C₆D₅)). ²H NMR of mixture (600 MHz, C₆H₆, 2 day reaction time): δ = 7.59 (s, $\Delta \nu_{1/2}$ = 2.5 Hz, possible Cp*₂ScD resonance), 1.92 (t, CH₂D, Cp* containing product, $J_{HD} = 2.17 \text{ Hz}$), 1.69 (t, CH₂D (Cp*₂ScPh), $J_{HD} = 2.19 \text{ Hz}$). Due to rapid H-D exchange with the C₆H₆ solvent, the signals for the deuterons of $Cp_2^*Sc(C_6D_5)$ were not observed.⁴¹

[K(crypt)][Cp"₂ScI], 5. In an argon-containing glovebox, Cp"₂ScI (25 mg, 0.05 mmol) and 2.2.2-cryptand (18 mg, 0.05 mmol) were dissolved in 4 mL of Et_2O and cooled to $-35\,^{\circ}C$ for 1 h. The solution was then pipetted into a scintillation vial containing KC₈ (7 mg, 0.05 mmol) precooled to -35 °C. An immediate color change from yellow to green-brown was observed. The solution was filtered through a Kimwipe-packed glass pipet to remove black solids, presumably graphite, and then placed in a -35 °C freezer for 3 h to yield dark redbrown block crystals of [K(crypt)][Cp"₂ScI] suitable for X-ray diffraction (39 mg, 86%). ATR-FTIR (cm⁻¹): 2951 (m), 2882. (m), 2786 (m), 2717 (m), 1444 (m), 1399 (w), 1360 (w), 1330 (w), 1296 (w), 1245 (s), 1212 (w), 1109 (s), 1079 (s), 978m, 952 (w), 922 (m), 828 (s), 799 (s, sh), 750 (s), 735 (s), 688 (s). UV-vis (Et₂O, 298 K) $\lambda_{\text{max}}/\text{nm}$ ($\varepsilon/$ M⁻¹cm⁻¹): 430 (1300). Magnetic moment (Evans method, THF, 190 K) = 1.5 $\mu_{\rm B}$. Anal. Calcd for ScC₄₀H₇₈N₂O₆Si₂KI: Sc 4.7; found: Sc 4.2.

Chelate-Free Reduction of Cp″₂ScI. In an argon-containing glovebox, Cp″₂ScI (25 mg, 0.05 mmol) was dissolved in 4 mL of Et₂O and chilled to -35 °C for 1 h. The solution was then pipetted into a scintillation vial containing KC₈ (7 mg, 0.05 mmol), also chilled to -35 °C. An immediate color change from yellow to green-brown was observed. The solution was filtered through a Kimwipe-packed glass pipet to remove black solids, presumably graphite, and then stored in a -35 °C freezer. UV–vis, $\lambda_{\rm max}/{\rm nm}$ (Et₂O, 298 K): 430.

[Cp*2Sc(18-Crown-6- κ^2 O,O')][Cp*2Sc₂], **6.** Cp*2ScI (0.050 g, 0.11 mmol) and 18-crown-6 (0.030 g, 0.11 mmol) were dissolved in ca. 5 mL of diethyl ether in a 20 mL vial, and the yellow solution was cooled to ca. -78 °C. KC₈ (0.017 g, 0.12 mmol) was added in one portion, and the mixture became dark red/brown. The mixture was then allowed to warm to ambient temperature and left to stand for 2 h. The solution was filtered, and the solvent was removed under reduced pressure. During this process, crystals of **6** which were suitable for X-ray diffraction had grown on the walls of the vial.

ASSOCIATED CONTENT

Supporting Information

The Supporting Information is available free of charge at https://pubs.acs.org/doi/10.1021/jacs.3c11922.

X-ray crystallography; EPR spectra; NMR spectra; infrared spectra; MALDI TOF mass spectra; UV-visible

spectra and decomposition kinetics data; and computational details (PDF)

Accession Codes

CCDC 2293719, 2294332—2294333, and 2294338—2294339 contain the supplementary crystallographic data for this paper. These data can be obtained free of charge via www.ccdc.cam.ac.uk/data_request/cif, or by emailing data_request@ccdc.cam.ac.uk, or by contacting The Cambridge Crystallographic Data Centre, 12 Union Road, Cambridge CB2 1EZ, UK; fax: +44 1223 336033.

AUTHOR INFORMATION

Corresponding Authors

Filipp Furche — Department of Chemistry, University of California, Irvine, California 92697-2025, United States; orcid.org/0000-0001-8520-3971; Email: filipp.furche@uci.edu

William J. Evans — Department of Chemistry, University of California, Irvine, California 92697-2025, United States; orcid.org/0000-0002-0651-418X; Email: wevans@uci.edu

Authors

Joshua D. Queen – Department of Chemistry, University of California, Irvine, California 92697-2025, United States;
orcid.org/0000-0002-6726-417X

Lauren M. Anderson-Sanchez — Department of Chemistry, University of California, Irvine, California 92697-2025, United States; orcid.org/0000-0002-9697-8008

Cary R. Stennett — Department of Chemistry, University of California, Irvine, California 92697-2025, United States; orcid.org/0000-0002-2727-5747

Ahmadreza Rajabi — Department of Chemistry, University of California, Irvine, California 92697-2025, United States; orcid.org/0000-0002-2188-762X

Joseph W. Ziller – Department of Chemistry, University of California, Irvine, California 92697-2025, United States;
orcid.org/0000-0001-7404-950X

Complete contact information is available at: https://pubs.acs.org/10.1021/jacs.3c11922

Notes

The authors declare no competing financial interest.

ACKNOWLEDGMENTS

We thank the U.S. National Science Foundation for support of this research under CHE-2154255 (to W.J.E. for the experimental research) and CHE-2102568 (to F.F. for the theoretical studies). We also thank Professor A. S. Borovik, Phan Phu, and Dr. Alec Follmer for assistance with the EPR spectroscopy and Joseph Q. Nguyen for help with the X-ray crystallography. The Eddleman Quantum Institute is acknowledged for learning and collaboration opportunities.

■ REFERENCES

- (1) Cloke, F. G. N.; Khan, K.; Perutz, R. N. η-Arene complexes of scandium(0) and scandium(II). *J. Chem. Soc., Chem. Commun.* **1991**, 1372–1373.
- (2) Cloke, F. G. N. Zero oxidation state compounds of scandium, yttrium, and the lanthanides. *Chem. Soc. Rev.* **1993**, 22, 17–24.
- (3) Arnold, P. L.; Cloke, F. G. N.; Hitchcock, P. B.; Nixon, J. F. The First Example of a Formal Scandium(I) Complex: Synthesis and Molecular Structure of a 22-Electron Scandium Triple Decker

- Incorporating the Novel 1,3,5-Triphosphabenzene Ring. J. Am. Chem. Soc. 1996, 118, 7630–7631.
- (4) Arnold, P. L.; Cloke, F. G. N.; Nixon, J. F. The first stable scandocene: synthesis and characterisation of $bis(\eta-2,4,5-tri-tert-butyl-1,3-diphosphacyclopentadienyl)scandium(II).$ *Chem. Commun.***1998**, 797–798.
- (5) Woen, D. H.; Chen, G. P.; Ziller, J. W.; Boyle, T. J.; Furche, F.; Evans, W. J. Solution Synthesis, Structure, and CO₂ Reduction Reactivity of a Scandium(II) Complex, {Sc[N(SiMe₃)₂]₃}-. Angew. Chem., Int. Ed. **2017**, 56, 2050–2053.
- (6) Moehring, S. A.; Beltrán-Leiva, M. J.; Páez-Hernández, D.; Arratia-Pérez, R.; Ziller, J. W.; Evans, W. J. Rare-Earth Metal(II) Aryloxides: Structure, Synthesis, and EPR Spectroscopy of [K(2.2.2-cryptand)][Sc(OC₆H₂^tBu₂-2,6-Me-4)₃]. *Chem.—Eur. J.* **2018**, 24, 18059–18067.
- (7) Fischer, E. O.; Pfab, W. Cyclopentadien-Metallkomplexe, ein neuer Typ metallorganischer Verbindungen. Z. Naturforsch. B 1952, 7, 377–379.
- (8) Wilkinson, G.; Rosenblum, M.; Whiting, M. C.; Woodward, R. B. The structure of iron bis-cyclopentadienyl. *J. Am. Chem. Soc.* 1952, 74, 2125–2126.
- (9) Sitzmann, H.; Dezember, T.; Schmitt, O.; Weber, F.; Wolmershäuser, G.; Ruck, M. metallocenes of Samarium, Europium, and Ytterbium with the Especially Bulky Cyclopentadienyl Ligands C₅H(CHMe₂)₄, C₅H₂(CMe₃)₃, and C₅(CHMe₂)₅. Z. Anorg. Allg. Chem. **2000**, 626, 2241–2244.
- (10) Gould, C. A.; McClain, K. R.; Yu, J. M.; Groshens, T. J.; Furche, F.; Harvey, B. G.; Long, J. R. Synthesis and Magnetism of Neutral, Linear Metallocene Complexes of Terbium(II) and Dysprosium(II). *J. Am. Chem. Soc.* **2019**, *141*, 12967–12973.
- (11) McClain, K. R.; Gould, C. A.; Marchiori, D. A.; Kwon, H.; Nguyen, T. T.; Rosenkoetter, K. E.; Kuzmina, D.; Tuna, F.; Britt, R. D.; Long, J. R.; Harvey, B. G. Divalent Lanthanide metallocene Complexes with a Linear Coordination Geometry and Pronounced 6s–5d Orbital Mixing. J. Am. Chem. Soc. 2022, 144, 22193–22201.
- (12) Brennan, J. G.; Cloke, F. G. N.; Sameh, A. A.; Zalkin, A. Synthesis of bis(η -1,3,5-tri-t-butylbenzene) sandwich complexes of yttrium(0) and gadolinium(0); the X-ray crystal structure of the first authentic lanthanide(0) complex, $[Gd(\eta-Bu^t_3C_6H_3)_2]$. J. Chem. Soc., Chem. Commun. 1987, 1668–1669.
- (13) Anderson, D. M.; Cloke, F. G. N.; Cox, P. A.; Edelstein, N.; Green, J. C.; Pang, T.; Sameh, A. A.; Shalimoff, G. On the stability and bonding in bis(η -arene)lanthanide complexes. *J. Chem. Soc., Chem. Commun.* **1989**, 53–55.
- (14) Jaroschik, F.; Nief, F.; Le Goff, X.-F.; Ricard, L. Isolation of Stable Organodysprosium(II) Complexes by Chemical Reduction of Dysprosium(III) Precursors. *Organometallics* **2007**, *26*, 1123–1125.
- (15) Jaroschik, F.; Momin, A.; Nief, F.; Le Goff, X.-F.; Deacon, G. B.; Junk, P. C. Dinitrogen Reduction and C—H Activation by the Divalent Organoneodymium Complex [(C₅H₂'Bu₃)₂Nd(μ-I)K([18]-crown-6)]. *Angew. Chem., Int. Ed.* **2009**, 48, 1117–1121.
- (16) Weber, F.; Schultz, M.; Sofield, C. D.; Andersen, R. A. Synthesis and Solid State Structures of Sterically Crowded d⁰-metallocenes of Magnesium, Calcium, Strontium, Barium, Samarium, and Ytterbium. *Organometallics* **2002**, *21*, 3139–3146.
- (17) Maron, L.; Werkema, E. L.; Perrin, L.; Eisenstein, O.; Andersen, R. A. Hydrogen for Fluorine Exchange in C₆F₆ and C₆F₅H by Monomeric [1,3,4-(Me₃C)₃C₅H₂]₂CeH: Experimental and Computational Studies. *J. Am. Chem. Soc.* **2005**, 127, 279–292.
- (18) Jaroschik, F.; Nief, F.; Ricard, L. Synthesis of a new stable, neutral organothulium(ii) complex by reduction of a thulium(iii) precursor. *Chem. Commun.* **2006**, 426–428.
- (19) Werkema, E. L.; Maron, L.; Eisenstein, O.; Andersen, R. A. Reactions of Monomeric $[1,2,4\cdot(Me_3C)_3C_5H_2]_2$ CeH and CO with or without H_2 : An Experimental and Computational Study. *J. Am. Chem. Soc.* **2007**, *129*, 2529–2541.
- (20) Werkema, E. L.; Yahia, A.; Maron, L.; Eisenstein, O.; Andersen, R. A. Bridging Silyl Groups in σ -Bond Metathesis and [1,2]-Shifts. Experimental and Computational Study of the Reaction between

- Cerium Metallocenes and MeOSiMe₃. Organometallics 2010, 29, 5103-5110.
- (21) Nocton, G.; Ricard, L. N-aromatic heterocycle adducts of bulky $[1,2,4-(Me_3C)_3C_5H_2]_2$ Sm: synthesis, structure and solution analysis. *Dalton Trans.* **2014**, 43, 4380–4387.
- (22) Goodwin, C. A. P.; Ortu, F.; Reta, D.; Chilton, N. F.; Mills, D. P. Molecular magnetic hysteresis at 60 K in dysprosocenium. *Nature* **2017**, *548*, 439–442.
- (23) Goodwin, C. A. P.; Reta, D.; Ortu, F.; Chilton, N. F.; Mills, D. P. Synthesis and Electronic Structures of Heavy Lanthanide Metallocenium Cations. J. Am. Chem. Soc. 2017, 139, 18714–18724.
- (24) Xémard, M.; Goudy, V.; Braun, A.; Tricoire, M.; Cordier, M.; Ricard, L.; Castro, L.; Louyriac, E.; Kefalidis, C. E.; Clavaguéra, C.; Maron, L.; Nocton, G. Reductive Disproportionation of CO₂ with Bulky Divalent Samarium Complexes. *Organometallics* **2017**, *36*, 4660–4668.
- (25) Guo, F.-S.; Day, B. M.; Chen, Y.-C.; Tong, M.-L.; Mansikkamäki, A.; Layfield, R. A. A Dysprosium metallocene Single-Molecule Magnet Functioning at the Axial Limit. *Angew. Chem., Int. Ed.* **2017**, *56*, 11445–11449.
- (26) Ortu, F.; Packer, D.; Liu, J.; Burton, M.; Formanuik, A.; Mills, D. P. Synthesis and structural characterization of lanthanum and cerium substituted cyclopentadienyl borohydride complexes. *J. Organomet. Chem.* **2018**, 857, 45–51.
- (27) Liptrot, D. J.; Power, P. P. London dispersion forces in sterically crowded inorganic and organometallic molecules. *Nat. Rev. Chem.* **2017**, *1*, 0004.
- (28) Mears, K. L.; Power, P. P. Beyond Steric Crowding: Dispersion Energy Donor Effects in Large Hydrocarbon Ligands. *Acc. Chem. Res.* **2022**, *55*, 1337–1348.
- (29) Sitzmann, H. Maximum spin cyclopentadienyl complexes of 3d transition metals. *Coord. Chem. Rev.* **2001**, *214*, 287–327.
- (30) Elschenbroich, C. Organometallics; Wiley, 2006.
- (31) Huynh, W.; Culver, D. B.; Tafazolian, H.; Conley, M. P. Solidstate ⁴⁵Sc NMR studies of Cp*₂Sc-X and Cp*₂ScX(THF). *Dalton Trans.* **2018**, 47, 13063–13071.
- (32) Pauling, L. The Nature of the Chemical Bond; Cornell University Press, 1960.
- (33) Stoll, S.; Schweiger, A. EasySpin, a comprehensive software package for spectral simulation and analysis in EPR. *J. Magn. Reson.* **2006**, *178*, 42–55.
- (34) Bain, G. A.; Berry, J. F. Diamagnetic Corrections and Pascal's Constants. *J. Chem. Educ.* **2008**, *85*, 532–536.
- (35) Evans, D. F. The determination of the paramagnetic susceptibility of substances in solution by nuclear magnetic resonance. *J. Chem. Soc.* **1959**, 2003–2005.
- (36) Sur, S. K. Measurement of magnetic susceptibility and magnetic moment of paramagnetic molecules in solution by high-field fourier transform NMR spectroscopy. *J. Magn. Reson.* **1989**, *82*, 169–173.
- (37) Shannon, R. D. Revised effective ionic radii and systematic studies of interatomic distances in halides and chalcogenides. *Acta Crystallogr.* **1976**, *A32*, 751–767.
- (38) Evans, W. J.; Kozimor, S. A.; Ziller, J. W. Methyl Displacements from Cyclopentadienyl Ring Planes in Sterically Crowded (C₅Me₅)₃M Complexes. *Inorg. Chem.* **2005**, *44*, 7960–7969.
- (39) Dawoodi, Z.; Green, M. L. H.; Mtetwa, V. S. B.; Prout, K.; Schultz, A. J.; Williams, J. M.; Koetzle, T. F. Evidence for carbon-hydrogen-titanium interactions: synthesis and crystal structures of the agostic alkyls [TiCl₃(Me₂PCH₂CH₂PMe₂)R](R = Et or Me). *J. Chem. Soc., Dalton Trans.* **1986**, 1629–1637.
- (40) Haaland, A.; Scherer, W.; Ruud, K.; McGrady, G. S.; Downs, A. J.; Swang, O. On the Nature and Incidence of β -agostic Interactions in Ethyl Derivatives of Early Transition Metals: Ethyltitanium Trichloride and Related Compounds. *J. Am. Chem. Soc.* **1998**, *120*, 3762–3772.
- (41) Thompson, M. E.; Baxter, S. M.; Bulls, A. R.; Burger, B. J.; Nolan, M. C.; Santarsiero, B. D.; Schaefer, W. P.; Bercaw, J. E. σ -Bond metathesis for carbon-hydrogen bonds of hydrocarbons and Sc-R (R = H, alkyl, aryl) bonds of permethylscandocene derivatives. Evidence

- for noninvolvement of the π system in electrophilic activation of aromatic and vinylic C-H bonds. *J. Am. Chem. Soc.* **1987**, 109, 203–219
- (42) Coles, M. P.; Hitchcock, P. B.; Lappert, M. F.; Protchenko, A. V. Syntheses and Structures of the Crystalline, Highly Crowded 1,3-Bis(trimethylsilyl)cyclopentadienyls [MCp"₃] (M = Y, Er, Yb), [PbCp"₂], [{YCp"₂(μ -OH)}₂], [(ScCp"₂)₂(μ - η ²: η ²-C₂H₄)], [YbCp"₂Cl(μ -Cl)K(18-crown-6)], and [{KCp"}_∞]. Organometallics **2012**, 31, 2682–2690.
- (43) Corbey, J. F.; Woen, D. H.; Palumbo, C. T.; Fieser, M. E.; Ziller, J. W.; Furche, F.; Evans, W. J. Ligand Effects in the Synthesis of Ln²⁺ Complexes by Reduction of Tris(cyclopentadienyl) Precursors Including C–H Bond Activation of an Indenyl Anion. *Organometallics* **2015**, *34*, 3909–3921.
- (44) Fieser, M. E.; Palumbo, C. T.; La Pierre, H. S.; Halter, D. P.; Voora, V. K.; Ziller, J. W.; Furche, F.; Meyer, K.; Evans, W. J. Comparisons of lanthanide/actinide + 2 ions in a tris(aryloxide)arene coordination environment. *Chem. Sci.* **2017**, *8*, 7424–7433.
- (45) Palumbo, C. T.; Halter, D. P.; Voora, V. K.; Chen, G. P.; Chan, A. K.; Fieser, M. E.; Ziller, J. W.; Hieringer, W.; Furche, F.; Meyer, K.; Evans, W. J. Metal versus Ligand Reduction in Ln³⁺ Complexes of a Mesitylene-Anchored Tris(Aryloxide) Ligand. *Inorg. Chem.* **2018**, *57*, 2823–2833.
- (46) Palumbo, C. T.; Halter, D. P.; Voora, V. K.; Chen, G. P.; Ziller, J. W.; Gembicky, M.; Rheingold, A. L.; Furche, F.; Meyer, K.; Evans, W. J. Using Diamagnetic Yttrium and Lanthanum Complexes to Explore Ligand Reduction and C–H Bond Activation in a Tris(aryloxide)mesitylene Ligand System. *Inorg. Chem.* **2018**, *57*, 12876–12884.
- (47) Jenkins, T. F.; Bekoe, S.; Ziller, J. W.; Furche, F.; Evans, W. J. Synthesis of a Heteroleptic Pentamethylcyclopentadienyl Yttrium(II) Complex, [K(2.2.2-Cryptand)]{(C_5Me_5)₂Y^{II}[N(SiMe₃)₂]}, and Its C–H Bond Activated Y(III) Derivative. *Organometallics* **2021**, 40, 3917–3925.
- (48) Brintzinger, H.; Bercaw, J. E. Nature of so-called titanocene, $(C_{10}H_{10}Ti)_2$. J. Am. Chem. Soc. **1970**, 92, 6182–6185.
- (49) Horáček, M.; Hiller, J.; Thewalt, U.; Polášek, M.; Mach, K. Activation of the (Trimethylsilyl)tetramethylcyclopentadienyl Ligand in the $[C_5Me_4(SiMe_3)]_2TiCl_2/Mg$ System, Yielding Intramolecular Si–CH₂–Mg and Si–CH₂–Ti Bonds. Molecular Structures of $\{[\eta^5-C_5Me_4SiMe_2(\mu-CH_2\{Mg_3Mg\})][\eta^5-C_5Me_4(SiMe_3)]Ti^{III}(\mu-H)_2Mg-(THF)\}_2$ and $[\eta^5:\eta^1-C_5Me_4SiMe_2CH_2][\eta^5-C_5Me_4(SiMe_3)]Ti^{III}$. Organometallics 1997, 16, 4185–4191.
- (50) Culver, D. B.; Huynh, W.; Tafazolian, H.; Ong, T.-C.; Conley, M. P. The β -agostic Structure in (C_5Me_5)₂Sc(CH_2CH_3): Solid-State NMR Studies of (C_5Me_5)₂Sc-R (R = Me, Ph, Et). *Angew. Chem., Int. Ed.* **2018**, *57*, 9520–9523.
- (51) Staroverov, V. N.; Scuseria, G. E.; Tao, J.; Perdew, J. P. Comparative assessment of a new nonempirical density functional: Molecules and hydrogen-bonded complexes. *J. Chem. Phys.* **2003**, *119*, 12129—12137.
- (52) Armbruster, M. K.; Weigend, F.; van Wüllen, C.; Klopper, W. Self-consistent treatment of spin-orbit interactions with efficient Hartree-Fock and density functional methods. *Phys. Chem. Chem. Phys.* **2008**, *10*, 1748–1756.
- (53) Grimme, S.; Antony, J.; Ehrlich, S.; Krieg, H. A consistent and accurate ab initio parametrization of density functional dispersion correction (DFT-D) for the 94 elements H-Pu. *J. Chem. Phys.* **2010**, 132, 154104.
- (54) Grimme, S.; Ehrlich, S.; Goerigk, L. Effect of the damping function in dispersion corrected density functional theory. *J. Comput. Chem.* **2011**, 32, 1456–1465.
- (55) Schäfer, A.; Horn, H.; Ahlrichs, R. Fully optimized contracted Gaussian basis sets for atoms Li to Kr. *J. Chem. Phys.* **1992**, *97*, 2571–2577.
- (56) Weigend, F.; Ahlrichs, R. Balanced basis sets of split valence, triple zeta valence and quadruple zeta valence quality for H to Rn: Design and assessment of accuracy. *Phys. Chem. Chem. Phys.* **2005**, *7*, 3297–3305.

- (57) Gulde, R.; Pollak, P.; Weigend, F. Error-Balanced Segmented Contracted Basis Sets of Double-ζ to Quadruple-ζ Valence Quality for the Lanthanides. *J. Chem. Theory Comput.* **2012**, *8*, 4062–4068.
- (58) Klamt, A.; Schüürmann, G. COSMO: a new approach to dielectric screening in solvents with explicit expressions for the screening energy and its gradient. *J. Chem. Soc., Perkin Trans.* **1993**, 2, 799–805.
- (59) Franzke, Y. J.; Holzer, C.; Andersen, J. H.; Begušić, T.; Bruder, F.; Coriani, S.; Della Sala, F.; Fabiano, E.; Fedotov, D. A.; Fürst, S.; Gillhuber, S.; Grotjahn, R.; Kaupp, M.; Kehry, M.; Krstić, M.; Mack, F.; Majumdar, S.; Nguyen, B. D.; Parker, S. M.; Pauly, F.; Pausch, A.; Perlt, E.; Phun, G. S.; Rajabi, A.; Rappoport, D.; Samal, B.; Schrader, T.; Sharma, M.; Tapavicza, E.; Treß, R. T.; Voora, V.; Wodyński, A.; Yu, J. M.; Zerulla, B.; Furche, F.; Hattig, C.; Sierka, M.; Tew, D. P.; Weigend, F. TURBOMOLE: Today and Tomorrow. *J. Chem. Theory Comput.* 2023, 19, 6859–6890.
- (60) Rajabi, A.; Grotjahn, R.; Rappoport, D.; Furche, F. A DFT perspective on organometallic lanthanide chemistry. *Dalton Trans.* **2024**, *53*, 410.
- (61) Lauher, J. W.; Hoffmann, R. Structure and chemistry of bis(cyclopentadienyl)-ML_n complexes. *J. Am. Chem. Soc.* **1976**, 98, 1729–1742.
- (62) MacDonald, M. R.; Ziller, J. W.; Evans, W. J. Synthesis of a Crystalline Molecular Complex of Y^{2+} , [(18-crown-6)K]-[($C_5H_4SiMe_3$)₃Y]. J. Am. Chem. Soc. **2011**, 133, 15914–15917.
- (63) Fang, M.; Lee, D. S.; Ziller, J. W.; Doedens, R. J.; Bates, J. E.; Furche, F.; Evans, W. J. Synthesis of the $(N_2)^{3-}$ Radical from Y^{2+} and Its Protonolysis Reactivity To Form $(N_2H_2)^{2-}$ via the Y[N- $(SiMe_3)_2]_3/KC_8$ Reduction System. J. Am. Chem. Soc. **2011**, 133, 3784–3787.
- (64) Moehring, S. A.; Miehlich, M.; Hoerger, C. J.; Meyer, K.; Ziller, J. W.; Evans, W. J. A Room-Temperature Stable Y(II) Aryloxide: Using Steric Saturation to Kinetically Stabilize Y(II) Complexes. *Inorg. Chem.* **2020**, *59*, 3207–3214.
- (65) Guzei, I. A.; Wendt, M. An improved method for the computation of ligand steric effects based on solid angles. *Dalton Trans.* **2006**, 3991–3999.
- (66) Boyde, N. C.; Chmely, S. C.; Hanusa, T. P.; Rheingold, A. L.; Brennessel, W. W. Structural Distortions in $M[E(SiMe_3)_2]_3$ Complexes (M = Group 15, f-Element; E = N, CH): Is Three a Crowd? *Inorg. Chem.* **2014**, 53, 9703–9714.
- (67) Kahan, R. J.; Farnaby, J. H.; Tsoureas, N.; Cloke, F. G. N.; Hitchcock, P. B.; Coles, M. P.; Roe, S. M.; Wilson, C. Sterically encumbered mixed sandwich compounds of uranium(III): Synthesis and reactivity with small molecules. *J. Organomet. Chem.* **2018**, 857, 110–122.
- (68) Anderson-Sanchez, L. M.; Yu, J. M.; Ziller, J. W.; Furche, F.; Evans, W. J. Room-Temperature Stable Ln(II) Complexes Supported by 2,6-Diadamantyl Aryloxide Ligands. *Inorg. Chem.* **2023**, *62*, 706–714.
- (69) Nguyen, J. Q.; Anderson-Sanchez, L. M.; Moore, W. N. G.; Ziller, J. W.; Furche, F.; Evans, W. J. Replacing Trimethylsilyl with Triisopropylsilyl Provides Crystalline $(C_5H_4SiR_3)_3$ Th Complexes of Th(III) and Th(II). Organometallics **2023**, 42, 2927–2937.
- (70) Hitchcock, P. B.; Kerton, F. M.; Lawless, G. A. The Elusive Titanocene. *J. Am. Chem. Soc.* **1998**, *120*, 10264–10265.
- (71) Walter, M. D.; Sofield, C. D.; Booth, C. H.; Andersen, R. A. Spin Equilibria in Monomeric Manganocenes: Solid-State Magnetic and EXAFS Studies. *Organometallics* **2009**, 28, 2005–2019.
- (72) Walter, M. D.; White, P. S. $[Cp'FeI]_2$ as convenient entry into iron-modified pincer complexes: bimetallic η^6 , κ^1 -POCOP-pincer iron iridium compounds. *New. J. Chem.* **2011**, *35*, 1842–1854.
- (73) Bauer, H.; Weismann, J.; Saurenz, D.; Färber, C.; Schär, M.; Gidt, W.; Schädlich, I.; Wolmerhäuser, G.; Sun, Y.; Harder, S.; Sitzmann, H. Chromocene, ferrocene, cobaltocene, and nickelocene derivatives with isopropyl and methyl or trimethylsilyl substituents. *J. Organomet. Chem.* **2016**, 809, 63–73.
- (74) Peters, M.; Baabe, D.; Maekawa, M.; Bockfeld, D.; Zaretzke, M. K.; Tamm, M.; Walter, M. D. Pogo-stick Iron and Cobalt Complexes:

- Synthesis, Structures, and Magnetic Properties. *Inorg. Chem.* **2019**, *58*, 16475–16486.
- (75) Goodwin, C. A. P.; Giansiracusa, M. J.; Greer, S. M.; Nicholas, H. M.; Evans, P.; Vonci, M.; Hill, S.; Chilton, N. F.; Mills, D. P. Isolation and electronic structures of derivatized manganocene, ferrocene, and cobaltocene anions. *Nat. Chem.* **2021**, *13*, 243–248.
- (76) Bercaw, J. E. Bis(pentamethylcyclopentadienyl)titanium(II) and its complexes with molecular nitrogen. *J. Am. Chem. Soc.* **1974**, 96, 5087–5095.
- (77) Fisher, J. M.; Piers, W. E.; Young, V. G., Jr Crystal Structure of (Pentamethylcyclopentadienyl)- $(\pi \cdot \eta^5 : \sigma \cdot \eta^1$ -tetramethylfulvene)-titanium(III). *Organometallics* **1996**, *15*, 2410–2412.
- (78) Evans, W. J.; Hughes, L. A.; Hanusa, T. P. Synthesis and X-ray Crystal Structures of Bis(pentamethylcyclopentadienyl) Complexes of Samarium and Europium: $(C_5Me_5)_2Sm$ and $(C_5Me_5)_2Eu$. Organometallics 1986, 5, 1285–1291.
- (79) Schäfer, S.; Kaufmann, S.; Rösch, E. S.; Roesky, P. W. Divalent metallocenes of the lanthanides a guideline to properties and reactivity. *Chem. Soc. Rev.* **2023**, *52*, 4006–4045.
- (80) Hollis, K. T.; Burdett, J. K.; Bosnich, B. Why Are Bis(pentamethylcyclopentadienyl) Complexes, [MCp*₂] of Calcium, Strontium, Barium, Samarium, Europium, and Ytterbium Bent? *Organometallics* **1993**, *12*, 3385–3386.
- (81) Timofeeva, T. V.; Lii, J.-H.; Allinger, N. L. Molecular Mechanics Explanation of the metallocene Bent Sandwich Structure. *J. Am. Chem. Soc.* **1995**, *117*, 7452–7459.
- (82) Pangborn, A. B.; Giardello, M. A.; Grubbs, R. H.; Rosen, R. K.; Timmers, F. J. Safe and Convenient Procedure for Solvent Purification. *Organometallics* **1996**, *15*, 1518–1520.
- (83) Evans, W. J.; Allen, N. T. Ketone Coupling with Alkyl Iodides, Bromides, and Chlorides Using Thulium Diiodide: A More Powerful Version of SmI₂(THF)x/HMPA. *J. Am. Chem. Soc.* **2000**, *122*, 2118–2119.
- (84) Batchu, N. K.; Regadio, M. Methodologies and Developments in the Analysis of REEs. In *Critical and Rare Earth Elements: Recovery from Secondary Resources*, Abhilash; Akcil, A., Ed.; Taylor & Francis Group, 2019; pp 365–373.
- (85) Přibil, R. Present state of complexometry—IV: Determination of rare earths. *Talanta* **1967**, *14*, 619–627.
- (86) Meyer, G.; Garcia, E.; Corbett, J. D. The Ammonium Chloride Route to Anhydrous Rare Earth Chlorides—The Example of YCl₃. *Inorg. Synth.* **1989**, 25, 146–150.
- (87) Harvey, M. J.; Hanusa, T. P.; Young, V. G. Formation and crystal structures of a monomer–dimer pair of mono-(cyclopentadienyl)calcium complexes, $[C_5(t-Bu)_3H_2]_2CaI(THF)_2$ and $\{[C_5(t-Bu)_3H_2]_2CaI(THF)\}_2$. J. Organomet. Chem. **2001**, 626, 43–48.